Received: 27 August 2022 | Accepted: 9 September 2023

DOI: 10.1002/fut.22461

RESEARCH ARTICLE

THE JOURNAL OF FUTURES MARKETS WILEY

Calibration in the "real world" of a partially specified stochastic volatility model

Lorella Fatone[1] | **Francesca Mariani**[2] | **Francesco Zirilli**[3]

[1]Dipartimento di Matematica, Università di Camerino, Camerino (MC), Italy

[2]Dipartimento di Scienze Economiche e Sociali, Università Politecnica delle Marche, Ancona (AN), Italy

[3]Dipartimento di Matematica "G.Castelnuovo", Università di Roma "La Sapienza", Roma (RM), Italy

Correspondence
Francesca Mariani, Dipartimento di Scienze Economiche e Sociali, Università Politecnica delle Marche, Piazzale Martelli 8, 60121 Ancona (AN), Italy.
Email: f.mariani@univpm.it

Abstract

We study the "real world" calibration of a partially specified stochastic volatility model, where the analytic expressions of the asset price drift rate and of the stochastic variance drift are not specified. The model is calibrated matching the observed asset log returns and the priors assigned by the investor. No option price data are used in the calibration. The priors chosen for the asset price drift rate and for the stochastic variance drift are those suggested by the Heston model. For this reason, the model presented can be considered as an "enhanced" Heston model. The calibration problem is formulated as a stochastic optimal control problem and solved using the dynamic programming principle. The model presented and the Heston model are calibrated using synthetic and Standard & Poor 500 (S&P500) data. The calibrated models are used to produce 6, 12, and 24 months in the future synthetic and S&P500 forecasts.

KEYWORDS

calibration, optimal control, stochastic volatility models

JEL CLASSIFICATION

C51, C61, G17

1 | INTRODUCTION

Stochastic volatility models are used to describe the dynamics of log returns (or of prices) of risky assets traded in the financial markets and to price options that have these assets as underlying. To be used in practical circumstances, the stochastic volatility models must be calibrated. The calibration problem is the problem of identifying in a class of models the model that "best fits" a given set of data. Usually, the data used in the calibration are asset log returns (or asset prices) and/or option prices observed in the financial markets and their observation times. When the model to be calibrated is specified (i.e., when the analytic expression of the functions involved in the model is given), the solution of the calibration problem consists of finding the values of the model parameters that give the "best fit" between the model and the data used in the calibration. Many different methods, depending on the meaning given to the expression "best fit", have been proposed to calibrate specified stochastic volatility models, for a review of them see Fatone et al. (2014) and the references therein. For example, in Mariani et al. (2008) and Fatone et al. (2008), the Heston model

(Heston, 1993) is calibrated maximizing a likelihood function using as data of the calibration asset log returns and option prices. Broadie et al. (2007) calibrate a square root stochastic volatility model with jumps. The volatility and the risk premia parameters of the model are found using a set of option price data. The remaining parameters are determined from a set of asset price data. Carmona and Xu (1997) consider an arbitrage-free stochastic volatility model. First, they reduce the number of model parameters that must be determined in the calibration and, later, using the relative entropy method, they calibrate the resulting "reduced" model. In the papers cited above and in most of the mathematical finance literature on the calibration problem the models that must be calibrated are specified. However, the calibration of partially specified stochastic volatility models has also been studied. For example, Nayak and Papanicolaou (2007) specify only partially the stochastic volatility model studied. In fact, they simply assume that in the model, that must be calibrated, the drift of the stochastic volatility is a fast mean reverting factor, and they leave undetermined the analytic expression of this mean reverting factor. In Nayak and Papanicolaou (2007), the calibration problem is formulated using option price data and is solved finding the volatility surface that matches the data and minimizes a relative entropy functional with respect to a given prior volatility surface chosen by the investor, according to his opinions and risk tolerance. That is, in Nayak and Papanicolaou (2007), the relative entropy method, used in the calibration of volatility surfaces by Avellaneda et al. (1997), is adapted to the problem of calibrating a partially specified stochastic volatility model. In Avellaneda et al. (1997) and Nayak and Papanicolaou (2007), the data of the calibration are option prices (and the corresponding observation times and asset prices). The models considered are calibrated in the "risk-neutral world". This is the subset of the admissible models made of the risk-neutral models. The risk-neutral models are defined as those where the asset price and the option prices discounted at the risk-free interest rate are martingales. The study of calibration problems in the risk-neutral world is motivated by the needs of the practitioners, that trade derivatives in the financial markets and is widely adopted in the mathematical finance literature. Note that the risk-neutral world of the stochastic volatility models of mathematical finance and, in particular, the risk-neutral world of the Heston model (Heston, 1993) are not sets that, once given the parameters of the asset price dynamic model, are made of a unique model, as it is in the case of Black and Scholes model. In fact, the risk-neutral world of the stochastic volatility models of mathematical finance is a set made of infinitely many distinct models. Usually, the risk-neutral models are parametrized by one or several risk premium parameters. In the financial industry the stochastic volatility models, calibrated in the risk-neutral world, can be used for several purposes, for example, they can be used to evaluate or to forecast option prices. However, in the risk-neutral world, the market price of the volatility risk remains undetermined. This means that a stochastic volatility model, calibrated in the risk-neutral world, cannot be used in several other applications, for example, in wealth management or portfolio optimization, where asset prices and log returns must be computed or forecasted. For these last purposes it is necessary to identify the dynamics of the asset price in the "real world", that is, it is necessary to calibrate the asset price dynamic model, using as data a set of asset log returns (or of asset prices) and their observation times. The models calibrated in the real world can be used to forecast asset log returns (or asset prices), as often required in wealth management and portfolio optimization.

In this paper we study the class of partially specified stochastic volatility models introduced by Wilmott (1998) and Gatheral (2006). In this class of models the asset price drift rate and the stochastic variance drift are functions of time, asset log return (or asset price), and stochastic variance, whose analytic expression is not specified before the calibration. In this sense, the models considered are partially specified. We present a calibration procedure that determines these functions using as data a set of observed asset log returns (or of observed asset prices) and their observation times. This is the announced "real world" calibration of a partially specified stochastic volatility model. The calibration procedure relies on the assumption that, even if investors have different opinions about future events and different risk tolerances, they agree on the data used in the calibration, since these data are (real or simulated) observations. That is, the data are (real or simulated) facts, they are not investor opinions. The calibrated model is obtained by determining the asset price drift rate and the stochastic variance drift that pursue in an "optimal" way the following goals: (i) the asset log returns implied by the model fit the observed asset log returns used as data, (ii) the asset price drift rate fits a reference drift rate, (iii) the stochastic variance drift fits a reference drift, and (iv) at the end of the investment period the asset log return fits a reference final asset log return. The reference asset price drift rate, stochastic variance drift, and final asset log return are the priors, used in the calibration, that are chosen by the investor according to his opinions and risk tolerance. In this paper the Heston model calibrated in the real world provides the first two of these priors. The third one, that is, the reference final asset log return, is chosen with a fitting procedure starting from the data of the calibration. With this choice of priors, the model resulting from the calibration is a kind of "enhanced" version of the Heston model. The probability measure associated with the calibrated model is the real world probability measure associated with the data and the priors used in the calibration. Moreover, with the previous

choice of priors, when the goals (i) and (iv) of the calibration are removed, the model, resulting as the solution of the calibration problem, is the Heston model, that has the priors used in the calibration as asset price drift rate and stochastic variance drift. The previous choice of priors is only illustrative, in fact many alternative choices are possible. For example, choices of priors suggested by the stochastic volatility models of mathematical finance different from the Heston model are possible. The calibrated models, obtained with these choices, can be interpreted as "enhanced" versions of the stochastic volatility models that have suggested the priors chosen. The previous calibration problem is formulated as a stochastic optimal control problem, whose control variables are the asset price drift rate and the stochastic variance drift and whose state variables are the asset log return (or the asset price) and the stochastic variance. The objective functional of this control problem is the expected value of minus a weighted sum (with positive weights) of the following addenda: (j) the time integral of the squared difference of the asset log returns implied by the model and a function that fits the observed asset log returns used as data, (jj) the time integral of the squared difference of the asset price drift rate and the reference asset price drift rate, (jjj) the time integral of the squared difference of the stochastic variance drift and the reference stochastic variance drift, and (jv) the squared difference of the asset log return (or of the asset price) at the end of the investment period and the reference final asset log return (or final asset price). Maximizing this functional, subject to the constraints given by the stochastic differential equations of the asset price dynamic model and by their auxiliary conditions, corresponds to pursuing the goals (i)–(iv) of the calibration stated above. The relative importance of these goals in the calibration is determined by the choice of the weights of the corresponding addenda in the objective functional. In the rest of the paper we refer to the model calibrated solving this optimal control problem as "optimal control model" (i.e., the oc model). The optimal control problem considered is solved using the dynamic programming principle. Its value function is determined by solving a final value problem for the Hamilton-Jacobi-Bellman equation. Assuming that the value function of the control problem is a polynomial of degree two in the state variables with time-dependent coefficients the solution of the final value problem for the Hamilton-Jacobi-Bellman equation considered is reduced to the solution of a final value problem for a system of Riccati ordinary differential equations. Introducing an auxiliary parameter, the system of Riccati differential equations is solved with a perturbation method. The time-dependent coefficients of the value function are approximated with truncated series in the auxiliary parameter evaluated in a suitable parameter value. The asset price drift rate and the stochastic variance drift, determined in this way, are approximate solutions of the calibration problem and are functions of time, asset log return (or asset price), and stochastic variance, expressed by explicit formulae that can be easily evaluated numerically. The dynamical equations, resulting from the solution of the calibration problem, imply that the asset price and the stochastic variance are fully coupled in the drift terms of the equations. Empirical evidence of the existence of a relation of this kind between asset price and volatility of the asset price is widely documented and studied in the statistical literature about financial data. French et al. (1987) and Campbell and Hentschel (1991) have shown the presence in the asset price of a volatility feedback effect, that is, they have shown that an increase in volatility results in falling asset prices. Moreover, Black (1976), Broadie et al. (2007), and Christie (1982) studied quantitatively the leverage effect in the relation between asset price and volatility of the asset price, in particular they have shown that when the asset price falls the volatility of the asset price rises. Aït-Sahalia et al. (2013) have estimated the leverage effect starting from high-frequency data. Finally, Baillie and De Gennaro (1990) have further investigated the statistical relation between asset price and volatility of the asset price by studying market data. Leverage and volatility feedback effects are associated with the presence of a negative correlation between asset price and volatility of the asset price. Note that the findings of French et al. (1987), Broadie et al. (2007), Christie (1982), Baillie and De Gennaro (1990), and Aït-Sahalia et al. (2013) must be carefully considered before being transferred from the variance or the volatility of an asset price observed in the financial market to the stochastic variance or the stochastic volatility of a stochastic volatility model. In fact, the stochastic variance and the stochastic volatility of a stochastic volatility model are related, but are not the variance and the volatility of the asset price of the stochastic volatility model dynamics. Despite the empirical evidence discussed above and the previous warning about its interpretation, in most of the stochastic volatility models of mathematical finance, and, in particular, in the Heston model, the dynamics of the stochastic variance (and the dynamics of the stochastic volatility) is independent of the asset price (and of the asset log return). This is a rather unnatural assumption that is, probably, a consequence of the fact that most of the stochastic volatility models of mathematical finance have been originally developed outside mathematical finance in engineering fields where the assumption was justified. More realistically, in the models considered here and, in particular, in the model resulting from the calibration procedure presented in Section 2 a more general relation between asset price and stochastic variance is allowed. This relation, at least in principle, is able to represent the empirical evidence discussed in French et al. (1987), Broadie et al. (2007), Christie (1982), Baillie and De Gennaro (1990), and Aït-Sahalia et al. (2013).

The model and the calibration procedure presented are tested in numerical experiments involving synthetic and real data. The real data studied are the daily closing values of the Standard & Poor 500 (S&P500) index of the New York Stock Exchange (NYSE) during the period January 2, 2009–January 4, 2018. Let us explain how the synthetic data considered are generated. First of all the Heston model is calibrated (in the real world) using as data the time series of the S&P500 daily closing values relative to the period January 2, 2009–January 4, 2018 and one trajectory of the calibrated Heston model is computed integrating numerically a suitable initial value problem (Andersen, 2008). In this way, a trajectory of daily asset prices is generated and, for simplicity, these prices are attributed to the time period January 2, 2009–January 4, 2018. This choice makes easier in the numerical experiments presented the comparison between synthetic data forecasts and real data forecasts. The simulated prices and the corresponding log returns are referred to as Heston model prices and Heston model log returns. In the numerical experiments with synthetic data the Heston model is calibrated using as data a window of 630 consecutive daily Heston model prices. The same choice is used in the calibration of the models with real data (i.e., S&P500 daily closing values). In the numerical experiments involving real data the asset price drift rate and the stochastic variance drift chosen as priors of the calibration problem, studied in this paper, are obtained calibrating in the real world the Heston model using as data of the calibration a window of 630 consecutive daily closing values of the S&P500 index, that is, a window of (approximately) 30 consecutive (calendar) months of the S&P500 daily data. The third prior, that is, the reference final asset log return, is determined using the (real or synthetic) data of the calibration and a fitting procedure explained in Section 3. With this choice of priors, we solve the optimal control problem corresponding to the calibration of the oc model using as data the monthly log returns of the data associated with a time window, made of (approximately) 30 consecutive (calendar) months (i.e., 630 consecutive trading days). We move the data windows used to calibrate the Heston and the oc models forward in time across the data set available (precisely we move the data windows forward in time 1 month at the time across a period of, respectively, 72, 66, and 55 months for the 6, 12, and 24 months in the future forecasts), discarding from the new window considered the data of the first month of the previous window and inserting in the new window the data of the next month after the end of the previous window. For each time period considered we use the corresponding data windows to calibrate the Heston and the oc models. The calibrated Heston and oc models are used to forecast the Heston model log return 6 months in the future and the S&P500 index log return 6, 12, and 24 months in the future, that is, 6, 12, and 24 months after the end of the data window used in the calibration. For each data window considered we compute the relative errors committed using the S&P500 index (or the Heston model price) forecasted with the Heston model or with the oc model instead of the S&P500 index observed at the NYSE (or the Heston model price) and we compute the statistics of these relative errors on the samples of the S&P500 index (or the Heston model price) forecasts available. The statistics of these errors shows that in the numerical experiments presented the oc model forecasts are of higher quality than the Heston model forecasts.

The robustness of the calibration procedures adopted is studied. For simplicity, this analysis is done using the synthetic data. In the Heston model case the vectors of the parameters, obtained from the calibration of the Heston model in each one of the 55 data time windows considered in the numerical experiments, are compared. The comparison shows that these parameter vectors change slightly from a data time window to the next one and that they remain always close to the parameter vector used to generate the data. This suggests that (in the numerical experiments presented) the Heston model calibration procedure is stable. Moreover, it shows that (in the numerical experiments presented) the choice of two of the (three) priors used in the oc model calibration procedure (i.e., the two priors taken from the calibrated Heston model) is robust. For the third prior used in the oc model calibration procedure a similar analysis gives the same result. The asset price and stochastic variance drift rates, obtained as a solution of the oc model calibration problem in the 55 data time windows considered, are studied. It is shown that they change slightly from a data time window to the next one and that they remain grouped together. This last finding shows that (in the numerical experiments presented) the oc model calibration procedure is stable.

Finally, a sensitivity analysis of the oc model calibration procedure is performed. As already done in the robustness analysis, this is done with the synthetic data. That is, in the 55 data time windows considered, the priors used in the oc model calibration are perturbed randomly, and the relative difference between the corresponding solutions of the oc model calibration problem is computed and studied.

The robustness and the sensitivity analyses can be repeated using the real data considered instead of the synthetic data, and give results analogous to those presented here.

Note that it may be possible to improve the quality of the forecasts obtained with the oc model by studying the time series of the differences between the oc model forecasted and the observed prices with the tools of data science and machine learning.

This study is organized as follows. In Section 2 the models considered, the calibration problem studied and its solution are presented. In Section 3 the calibration procedure introduced in Section 2 is tested and some numerical experiments using synthetic and real data are discussed. Finally, in Section 4 some conclusions are drawn. In Appendix A some useful formulae are listed. In Appendix B the quantitative results obtained in the robustness and sensitivity analyses of the calibration procedures are shown.

2 | THE CALIBRATION PROCEDURE

Let n be a positive integer, $\mathbb{R}$, $\mathbb{R}_+$ be, respectively, the sets of real numbers and of positive real numbers, $\mathbb{R}^n$ be the n-dimensional real Euclidean space of column vectors and $\underline{x} = [x_1, x_2, ..., x_n]^\top \in \mathbb{R}^n, x_i \in \mathbb{R}, i = 1, 2, ..., n$, where $\cdot^\top$ denotes the transpose of $\cdot$, be a vector of $\mathbb{R}^n$. Moreover, let $T > 0$ be the time horizon of the investor, $[0, T]$ be a time interval called investment period, and $t \in [0, T]$ be a real variable that denotes time. We consider the following class of stochastic volatility models: in a market made of a risky asset let $S(t)$ be a random variable, that represents the price of the risky asset at time $t, t \in [0, T]$, the stochastic process $S(t), t \in [0, T]$, is defined by the following system of stochastic differential equations:

$$dS(t) = S(t)\tilde{f}_1(t, S(t), v(t))dt + S(t)\sqrt{v(t)}\,dB(t), \quad t \in [0, T], \tag{1}$$

$$dv(t) = \tilde{f}_2(t, S(t), v(t))dt + \sigma\sqrt{v(t)}\,dZ(t), \quad t \in [0, T], \tag{2}$$

with the initial conditions

$$S(0) = S_0, \tag{3}$$

$$v(0) = v_0. \tag{4}$$

The stochastic processes $B(t), Z(t), t \in [0, T]$, are standard Wiener processes, such that $B(0) = Z(0) = 0$ and their stochastic differentials $dB(t), dZ(t), t \in [0, T]$, are such that

$$\mathbb{E}^{\mathbb{P}}\{dB(t)dZ(t)\} = \rho dt, \quad t \in [0, T], \tag{5}$$

where $\mathbb{E}^{\mathbb{P}}\{\cdot\}$ denotes the expected value with respect to the measure $\mathbb{P}$ of $\cdot$ and $\rho \in \mathbb{R}$ such that $-1 < \rho < 1$, is a correlation coefficient. The auxiliary condition (5) completes the initial value problem (1)–(4). Hereafter, we refer to the Heston model (1)–(5) as Model 1. The measure $\mathbb{P}$ is the probability measure whose density is the transition probability function of Model 1. The random variable $v(t)$ defined through Model 1 is the stochastic variance of the asset price $S(t)$ at time $t, t \in [0, T]$. The stochastic variance $v(t)$ is an "auxiliary" variable, used to model the dynamics of the asset price $S(t), t \in [0, T]$, through Model 1, and it is not observable in the financial markets. In particular, the initial stochastic variance v_0 of (4) is not observable. The square root of $v(t)$ is the stochastic volatility of $S(t), t \in [0, T]$. In (1) and (2), σ is a real parameter called vol of vol, such that $\sigma \neq 0$, and $\tilde{f}_1 : [0, T] \times \mathbb{R}_+ \times \mathbb{R}_+ \to \mathbb{R}, \tilde{f}_2 : [0, T] \times \mathbb{R}_+ \times \mathbb{R}_+ \to \mathbb{R}$, are real functions called, respectively, asset price drift rate and stochastic variance drift. The analytic expression of the functions $\tilde{f}_1, \tilde{f}_2$ is not specified before the calibration of the model. In this sense, Model 1 is partially specified. However, the functions $\tilde{f}_1, \tilde{f}_2$ must satisfy some regularity and growth hypotheses to guarantee that Model 1 has a unique solution defined for $t \in [0, T]$. To avoid technicalities, these hypotheses are omitted. The random variables S_0, v_0 of (3) and (4) are the initial condition of (1) and (2) and we assume that these random variables are concentrated, respectively, in the points S_0, v_0 with probability one. We assume $S_0 > 0, v_0 > 0$. Note that, abusing the notation, S_0, v_0 denote both the random variables on the right-hand side of (3) and (4) and the points where these random variables are concentrated. The initial asset price S_0 is observable and in the calibration problems discussed in Sections 2 and 3 is assumed known. The initial stochastic variance v_0 is not observable and is an unknown parameter that must be assigned or determined in the calibration of the model.

The random variable $x(t) = \ln\left(\frac{S(t)}{S_0}\right)$, where $\ln(\cdot)$ denotes the logarithm of $\cdot$, is the asset log return at time $t, t \in [0, T]$. Note that, to avoid troubles, in the definition of $x(t)$ it is necessary that $S(t)$ is positive with probability one, $t \in [0, T]$. The functions $\tilde{f}_1, \tilde{f}_2$, rewritten as functions of time, asset log return, and stochastic variance (see Equations (6) and (7)) are the control variables and the stochastic processes $x(t), v(t), t \in [0, T]$, are the state variables of the stochastic optimal control problem that is used to formulate the real world calibration problem of Model 1. The class of stochastic volatility models, considered in the calibration problem, is defined by Model 1. A model in this class is calibrated when the functions $\tilde{f}_1, \tilde{f}_2$ and the parameters σ, ρ, v_0 are determined. In the calibration problem, studied in this section, the parameters σ, ρ, v_0 are assumed to be given. In this case, solving the calibration problem simply consists in determining the functions $\tilde{f}_1, \tilde{f}_2$, and this is done solving the stochastic optimal control problem presented below. In the numerical experiments, presented in Section 3, the value of the parameters σ, ρ, v_0 is not assigned it is determined calibrating the Heston model starting from a suitable data set. The data set, used in the calibration problem studied in this section, is a time series of observed asset log returns (or of observed asset prices). The measure $\mathbb{P}$, associated with the calibrated model, is the real world probability measure associated with the data and to the priors involved in the calibration.

Note that when $\tilde{f}_1(t, S, v) = \mu, \tilde{f}_2(t, S, v) = k(\theta - v), t \in [0, T], S, v \in \mathbb{R}_+$, with $\mu \in \mathbb{R}, k, \theta \in \mathbb{R}_+$ and in (1) and (2) $\sigma \neq 0$ is such that $\frac{2k\theta}{\sigma^2} > 1$, Model 1 reduces to the Heston model (Heston, 1993). The assumption $v_0 > 0$ with probability one, the choice $\tilde{f}_2(t, S, v) = k(\theta - v), t \in [0, T], S, v \in \mathbb{R}_+$, with $k, \theta \in \mathbb{R}_+$, in (2), Equations (2) and (4), $\sigma \neq 0$ and the condition $\frac{2k\theta}{\sigma^2} > 1$ derived by Feller (1951), imply that $v(t) > 0$ with probability one, $t \in [0, T]$. Moreover, the assumption $S_0 > 0$ with probability one, the choice $\tilde{f}_1(t, S, v) = \mu, t \in [0, T], S, v \in \mathbb{R}_+$, with $\mu \in \mathbb{R}$, in (1), $\tilde{f}_2(t, S, v) = k(\theta - v), t \in [0, T], S, v \in \mathbb{R}_+$, with $k, \theta \in \mathbb{R}_+, \sigma \neq 0$, in (2), the Feller condition $\frac{2k\theta}{\sigma^2} > 1, v_0 > 0$, and Model 1 imply that $S(t) > 0$ with probability one, $t \in [0, T]$. That is, in the Heston model, the assumption $S_0 > 0, v_0 > 0$ with probability one and the Feller condition $\frac{2k\theta}{\sigma^2} > 1, k, \theta \in \mathbb{R}_+, \sigma \neq 0$ imply $S(t) > 0, v(t) > 0$ with probability one, $t \in [0, T]$. In the Heston model the positivity of $v(t)$ with probability one is necessary to avoid the troubles due to the term $\sqrt{v(t)}$ in the model equations, $t \in [0, T]$.

From Model 1 and the definition of $x(t), t \in [0, T]$, it is easy to see that $x(t), v(t), t \in [0, T]$, satisfy the following system of stochastic differential equations:

$$dx(t) = \left(f_1(t, x(t), v(t)) - \frac{1}{2}v(t)\right)dt + \sqrt{v(t)}\,dB(t), \quad t \in [0, T], \tag{6}$$

$$dv(t) = f_2(t, x(t), v(t))dt + \sigma\sqrt{v(t)}\,dZ(t), \quad t \in [0, T], \tag{7}$$

with the initial conditions (3) and (4), where in (6) and (7) we have $f_1(t, x, v) = \tilde{f}_1(t, S_0e^x, v), t \in [0, T]$, $x \in \mathbb{R}, v \in \mathbb{R}_+, f_2(t, x, v) = \tilde{f}_2(t, S_0e^x, v), t \in [0, T], x \in \mathbb{R}, v \in \mathbb{R}_+$. Moreover, the initial condition (3), written for the asset price $S(0)$, is rewritten for the asset log return $x(0)$ as follows:

$$x(0) = 0. \tag{8}$$

Hereafter, for convenience, we refer to the oc model (6), (7), (8), (4), and (5) as Model 2. Using the asset log return $x(t), t \in [0, T]$, instead of the asset price $S(t), t \in [0, T]$, as the dependent variable Model 1 is rewritten as Model 2. Note that, going from the first to the second formulation of the model equation, (5) must be slightly reinterpreted, in fact, the change of dependent variable from $S(t), t \in [0, T]$, to $x(t), t \in [0, T]$, made in the model equations, must be reflected in the measure $\mathbb{P}$ of (5). However, for simplicity, the same symbol $\mathbb{P}$ is used to denote the measures of these two models. In the models considered, depending on the choice of the functions $\tilde{f}_1, \tilde{f}_2$ in (1) and (2), and from the (consequent) choice of the functions f_1, f_2 in (6) and (7), it may happen that during the time evolution the stochastic variance $v(t), t \in [0, T]$, that at time $t = 0$ is equal to the positive value v_0 with probability one, becomes negative with positive probability. This must be avoided. In fact, the intuitive meaning of stochastic variance and the presence of the term $\sqrt{v(t)}, t \in [0, T]$, in (1) and (2), and in (6) and (7), require the positivity of the stochastic variance (with probability one) for $t \in [0, T]$. This means that, when necessary, Models 1 and 2 must be equipped with a reflecting

condition to prevent the possibility of the event: "negative stochastic variance with positive probability" during the time evolution. In the models under investigation the reflecting condition has the role that the Feller condition $\frac{2k\theta}{\sigma^2} > 1, k, \theta \in \mathbb{R}_+, \sigma \neq 0$, has in the Heston model. More precisely, when necessary, a reflecting condition is imposed on the set $\{[x, v]^\top \in \mathbb{R}^2 \mid v = \epsilon\}$, where $\epsilon > 0$ is a given small number. The condition is imposed on the paths of $x(t), v(t), t \in [0, T]$ (or, similarly, on the paths of $S(t), v(t), t \in [0, T]$, when Model 1 is used) and guarantees that whenever a path of $v(t), t \in [0, T]$, coming from the region $v > \epsilon$ tries to cross the boundary $v = \epsilon$ to go in the region $v < \epsilon$ it bounces back (in a convenient way) into the region $v > \epsilon$. The reflecting condition is imposed in $v = \epsilon, \epsilon > 0$, instead of being imposed in $v = 0$, as it should be, since the point $v = 0$ is a singular point of (1) and (2), and of (6) and (7) due to the presence in these equations of the term $\sqrt{v(t)}, t \in [0, T]$, while the point $v = \epsilon$ is a regular point of (1) and (2) and of (6) and (7). That is, imposing the reflecting condition in $v = 0$ may generate mathematical subtleties of the same kind as those studied by Feller (1951) and, for simplicity, we prefer to avoid these subtleties here. In the sequel after imposing to Models 1 and 2, the reflecting condition in $v = \epsilon$, we assume $v_0 \in \mathbb{R}_\epsilon = \{v \in \mathbb{R} \mid v > \epsilon\}$. The reflecting condition imposed is explained in Section 3.

Often, the Feller condition is imposed to prevent difficulties with the interpretation of the Heston model. In fact, this condition ensures the strict positivity of the stochastic variance during the time evolution, and guarantees the unique solvability and well-posedness of the initial value problem for the Heston model. However, the Feller condition is only a sufficient condition for the positivity of the stochastic variance and, sometimes, in the calibration of the Heston model practitioners working with real data, ignore (and eventually violate) it. Actually, there could be some benefits in relaxing (and eventually violating) the Feller condition, as suggested in Amengual and Xiu (2018), Andersen and Piterbarg (2007), Pacati et al. (2018), and Song and Xiu (2016). In the oc model the reflecting condition imposed in Section 3 plays the same role as the Feller condition in the Heston model. In fact, the reflecting condition guarantees the positivity of the stochastic variance during the time evolution and the probabilistic interpretation of the oc model. More specifically, the reflecting condition guarantees that difficulties, due to the "destruction of probability", during the time evolution induced by the oc model are avoided. However, it must be pointed out that in the numerical experiments discussed in Section 3, rarely the reflecting condition is active. That is, in the numerical experiments presented, the reflecting condition imposed on the oc model can be removed without causing too much trouble for practical purposes.

Let $f_1^0(t, x, v) = \mu, f_2^0(t, x, v) = k(\theta - v), t \in [0, T], x \in \mathbb{R}, v \in \mathbb{R}_\epsilon, \mu \in \mathbb{R}, k, \theta \in \mathbb{R}_+$, be, respectively, the reference asset price drift rate and the reference stochastic variance drift chosen by the investor as priors of the calibration problem. This choice of f_1^0, f_2^0 is inspired by the Heston model. In fact, the functions f_1^0, f_2^0 chosen are, respectively, the asset price drift rate and the stochastic variance drift of the Heston model. Note that, in the functions f_1^0, f_2^0 chosen as priors of the calibration problem, the quantities μ, k, θ are not parameters, in fact, their numerical value must be given. In Section 3 the numerical values of the parameters μ, k, θ and those of v_0, ρ, σ, that are employed in the numerical experiments are determined by calibrating the Heston model starting from a suitable data set. Here, we assume that the numerical values of μ, k, θ are given. The random variable x_T denotes the reference asset log return at time $t = T$ and is a prior of the calibration. For simplicity, x_T is assumed to be concentrated in a point with probability one and, abusing the notation, the same symbol x_T is used to denote both the random variable and the point where the random variable is concentrated. In the experiments presented in Section 3, x_T is chosen using a set of observed asset log returns and a fitting procedure, here, we assume x_T given. The previous choice of the priors f_1^0, f_2^0, x_T is only illustrative. Many other choices are possible. In particular choices of f_1^0, f_2^0, inspired by the stochastic volatility models of mathematical finance different from the Heston model, are possible.

Let m be a positive integer, for $i = 1, 2, ..., m$ let $\tilde{x}_i$ be the asset log return observed at time $t = t_i$, where $0 < t_1 < t_2 < ... < t_m = T_1 < T$ are m observation times. Let $\tilde{x}(t), t \in [0, T]$, be a function determined with the (weighted) least-squares method that fits the m points $(t_i, \tilde{x}_i), i = 1, 2, ..., m$, and, eventually, some extra points obtained solving one or several auxiliary problems. In Section 3 we explain the choice of the function $\tilde{x}(t), t \in [0, T]$, done in the numerical experiments presented. The goal pursued by the investor in the calibration of Model 2 is the maximization of the objective functional, given by minus the expected value of a weighted sum (with positive weights) of the following quantities: (a) $\int_0^T (x(t) - \tilde{x}(t))^2 dt$, (b) $\int_0^T (f_1(t, x(t), v(t)) - \mu)^2 dt$, and (c) $\int_0^T (f_2(t, x(t), v(t)) - k(\theta - v(t)))^2 dt$, and (d) $-(x(T) - x_T)^2$, subject to the dynamical constraints (6) and (7) and to their initial and auxiliary conditions (8), (4), and (5). Given the choice of the priors done above, it is easy to see that the maximization of the previous objective functional corresponds to pursuing the goals of the calibration (i)–(iv) stated in Section 1.

Let us define the optimal control problem used to calibrate in the real world Model 2 when the previous choice of the priors f_1^0, f_2^0 is done and the parameters $\mu, k, \theta, v_0, \rho, \sigma$ and the prior x_T are given. Let $L^2([0,T])$ be the set of the square integrable real stochastic processes defined on the interval $[0,T]$, and the weights $w_i > 0$, $i = 1, 2, ..., 4$, be real constants such that $\sum_{i=1}^4 w_i = 1$, the real world calibration problem of Model 2 is formulated as the following stochastic optimal control problem:

$$\max_{f_1,f_2\in L^2([0,T])} \mathbb{E}^{\mathbb{P}}\Big\{-\frac{1}{2}\int_0^T [w_1(x(t)-\tilde{x}(t))^2 + w_2(f_1(t,x(t),v(t))-\mu)^2 + w_3((f_2(t,x(t),v(t))-k(\theta-v(t)))^2]\,dt - \frac{w_4}{2}(x(T)-x_T)^2\Big\}, \tag{9}$$

subject to Model 2. The choice of the positive weights w_i, $i = 1, 2, ..., 4$, is used to "balance" in the functional (9) the goals (i)–(iv) stated in Section 1 and pursued in the calibration, respectively, through the quantities (a)–(d) defined above. The choice of the weights w_i, $i = 1, 2, ..., 4$, done in the numerical experiments is explained in Section 3. The calibration problem formulated for Model 2 can be easily adapted to Model 1. For simplicity this is omitted. Hereafter, we refer to the optimal control problems (9), (6), (7), (8), (4), and (5) as Problem 1.

Problem 1 is solved using the dynamic programming principle. Let $V(t,x,v)$, $t \in [0,T]$, $x \in \mathbb{R}$, $v \in \mathbb{R}_\epsilon$, be the value function of Problem 1 defined as follows:

$$\begin{aligned} V(t,x,v) = \max_{f_1,f_2\in L^2([0,T])} \mathbb{E}^{\mathbb{P}}\Big\{&-\frac{1}{2}\int_t^T [w_1(x(s)-\tilde{x}(s))^2 + w_2(f_1(s,x(s),v(s))-\mu)^2 \\ &+ w_3(f_2(s,x(s),v(s))-k(\theta-v(s)))^2]\,t\,ds - \frac{w_4}{2}(x(T)-x_T)^2, \Big|\, x(t)=x, v(t)=v\Big\}, \\ &t\in[0,T],\quad x\in\mathbb{R},\quad v\in\mathbb{R}_\epsilon. \end{aligned} \tag{10}$$

In (10) and in the sequel we assume that the reflecting condition in $v = \epsilon$ is imposed.

The function $V(t,x,v)$, $t \in [0,T]$, $x \in \mathbb{R}$, $v \in \mathbb{R}_\epsilon$, defined in (10), satisfies the following Hamilton-Jacobi-Bellman equation (Kolosov, 1999):

$$\begin{aligned} &\frac{\partial V}{\partial t} - \frac{1}{2}v\frac{\partial V}{\partial x} + \frac{1}{2}v\frac{\partial^2 V}{\partial x^2} + \frac{1}{2}\sigma^2 v\frac{\partial^2 V}{\partial v^2} + \sigma\rho v\frac{\partial^2 V}{\partial x\partial v} - \frac{w_1}{2}(x-\tilde{x})^2 \\ &\quad + \max_{\psi_1,\psi_2\in\mathbb{R}}\Big(\psi_1\frac{\partial V}{\partial x} + \psi_2\frac{\partial V}{\partial v} - \frac{1}{2}w_2(\psi_1-\mu)^2 - \frac{1}{2}w_3(\psi_2-k(\theta-v))^2\Big) = 0, \\ &\quad t\in[0,T],\quad x\in\mathbb{R},\quad v\in\mathbb{R}_\epsilon, \end{aligned} \tag{11}$$

and the final condition

$$V(T,x,v) = -\frac{w_4}{2}(x-x_T)^2, \quad x\in\mathbb{R},\quad v\in\mathbb{R}_\epsilon. \tag{12}$$

Moreover, it is well known that the optimal control f_1^*, f_2^* solution of Problem 1, is given by (see Kolosov, 1999):

$$f_1^*(t,x,v) = \frac{1}{w_2}\frac{\partial V}{\partial x}(t,x,v) + \mu,\ t\in[0,T],\quad x\in\mathbb{R},\quad v\in\mathbb{R}_\epsilon, \tag{13}$$

$$f_2^*(t,x,v) = \frac{1}{w_3}\frac{\partial V}{\partial v}(t,x,v) + k(\theta-v),\ t\in[0,T],\quad x\in\mathbb{R},\quad v\in\mathbb{R}_\epsilon. \tag{14}$$

It is easy to see that

$$\max_{\psi_1,\psi_2\in\mathbb{R}}\left(\psi_1\frac{\partial V}{\partial x}+\psi_2\frac{\partial V}{\partial v}-\frac{1}{2}w_2(\psi_1-\mu)^2-\frac{1}{2}w_3(\psi_2-k(\theta-v))^2\right)$$
$$=\frac{1}{2w_3}\left(\frac{\partial V}{\partial v}\right)^2+\frac{1}{2w_2}\left(\frac{\partial V}{\partial x}\right)^2+k(\theta-v)\frac{\partial V}{\partial v}+\mu\frac{\partial V}{\partial x}. \tag{15}$$

Substituting (15) in (11) we have

$$\frac{\partial V}{\partial t}+\left(\mu-\frac{1}{2}v\right)\frac{\partial V}{\partial x}+\frac{1}{2}v\frac{\partial^2 V}{\partial x^2}+\frac{1}{2}\sigma^2 v\frac{\partial^2 V}{\partial v^2}+\sigma\rho v\frac{\partial^2 V}{\partial x\partial v}-\frac{w_1}{2}(x-\tilde{x})^2$$
$$+\frac{1}{2w_3}\left(\frac{\partial V}{\partial v}\right)^2+k(\theta-v)\frac{\partial V}{\partial v}+\frac{1}{2w_2}\left(\frac{\partial V}{\partial x}\right)^2=0,\quad t\in[0,T],\quad x\in\mathbb{R},\quad v\in\mathbb{R}_\epsilon, \tag{16}$$

and problem (11) and (12) becomes problem (16) and (12).

First of all, let us consider a limit case of problem (16) and (12) corresponding to the choice of the weights $w_1=w_4=0, w_2>0, w_3>0$. This corresponds to removing the terms (a) and (d) from the objective functional (9) and, as a consequence, to removing the goals (i) and (iv) from the calibration procedure. It is easy to see that in this limit case the optimal control f_1^*, f_2^* determined solving problem (16) and (12), is given by the asset price drift rate and the stochastic variance drift of the Heston model, that have been used as priors in the formulation of the calibration problem. This last fact shows one interesting aspect of the relation between the Heston model and the model presented here. In fact, when $w_1=w_4=0, w_2>0, w_3>0$ problem (16) and (12) reduces to equation:

$$\frac{\partial V}{\partial t}+\left(\mu-\frac{1}{2}v\right)\frac{\partial V}{\partial x}+\frac{1}{2}v\frac{\partial^2 V}{\partial x^2}+\frac{1}{2}\sigma^2 v\frac{\partial^2 V}{\partial v^2}+\sigma\rho v\frac{\partial^2 V}{\partial x\partial v}+\frac{1}{2w_3}\left(\frac{\partial V}{\partial v}\right)^2$$
$$+k(\theta-v)\frac{\partial V}{\partial v}+\frac{1}{2w_2}\left(\frac{\partial V}{\partial x}\right)^2=0,\quad t\in[0,T],\quad x\in\mathbb{R},\quad v\in\mathbb{R}_\epsilon, \tag{17}$$

with the final condition

$$V(T,x,v)=0,\quad x\in\mathbb{R},\quad v\in\mathbb{R}_\epsilon. \tag{18}$$

The function $V(t,x,v)=0, t\in[0,T], x\in\mathbb{R}, v\in\mathbb{R}_\epsilon$ is a solution of (17) and (18). That is, from (13) and (14) it follows that when $w_1=w_4=0, w_2>0, w_3>0$ the value function, solution of (17) and (18), is $V(t,x,v)=0, t\in[0,T], x\in\mathbb{R}, v\in\mathbb{R}_+$, and the optimal control f_1^*, f_2^* of Problem 1 is

$$f_1^*(t,x,v)=\mu,\quad t\in[0,T],\quad x\in\mathbb{R},\quad v\in\mathbb{R}_\epsilon, \tag{19}$$

$$f_2^*(t,x,v)=k(\theta-v),\quad t\in[0,T],\quad x\in\mathbb{R},\quad v\in\mathbb{R}_\epsilon. \tag{20}$$

That is, in the limit case studied, the optimal control found f_1^*, f_2^*, given by (19) and (20), are the asset price drift rate and the stochastic variance drift of the Heston model, that have been chosen as priors f_1^0, f_2^0 in the formulation of the calibration problem. In this case, when the Feller condition $\frac{2k\theta}{\sigma^2}>1, k,\theta\in\mathbb{R}_+, \sigma\neq 0$, holds the reflecting condition imposed in $v=\epsilon$ is not needed. In the previous circumstances, the model, resulting from the solution of Problem 1 when $w_1=w_4=0, w_2>0, w_3>0$, is the Heston model that has the priors chosen in the formulation of the calibration problem as asset price drift rate and stochastic variance drift. It is easy to see that by choosing appropriately the priors f_1^0, f_2^0 it is possible to obtain as special cases of calibration problems analogous to Problem 1 the other stochastic volatility models of mathematical finance of common use. Note that when $w_1=w_4=0, w_2>0, w_3>0$ the intervention of the data in Problem 1 is limited to the determination of the numerical values of $\mu, k, \theta, v_0, \rho, \sigma$. In fact, these parameters, that, for simplicity, are assumed given here, in Section 3 are determined from a suitable set of data calibrating the Heston model. That is, when $w_1=w_4=0,\ w_2>0, w_3>0$, proceeding as done in Section 3 the calibration of the oc model reduces to the calibration of the Heston model. Let us consider Problem 1 when

$w_i > 0, i = 1, 2, ..., 4$, and let us seek a solution for the final value problem (16) and (12) corresponding Hamilton-Jacobi-Bellman equation of the form

$$V(t,x,v) = \alpha(t) + \beta(t)v + \gamma(t)v^2 + \delta(t)xv + \varepsilon(t)x + \varphi(t)x^2, t \in [0,T], x \in \mathbb{R}, v \in \mathbb{R}_\epsilon, \tag{21}$$

where $\alpha(t), \beta(t), \gamma(t), \delta(t), \varepsilon(t), \varphi(t), t \in [0,T]$, are real functions to be determined. Substituting (21) in (16) and (12) and using the polynomial identity principle, it is easy to see that the value function V, given by (21), solves (16) and (12) if $\underline{h}(t) = [\alpha(t), \beta(t), \gamma(t), \delta(t), \varepsilon(t), \varphi(t)]^\top \in \mathbb{R}^6, t \in [0,T]$, solves the final value problem:

$$\frac{d\underline{h}(t)}{dt} = D\underline{h}(t) + E(\underline{h}(t))\underline{h}(t) + \underline{b}(t), \quad t \in [0,T], \tag{22}$$

$$\underline{h}(T) = w_4\left[-\frac{1}{2}x_T^2, 0, 0, 0, x_T, -\frac{1}{2}\right]^\top, \tag{23}$$

where $D, E(\underline{k})$ are 6×6 matrices defined in (A1) and (A2), $\underline{k} \in \mathbb{R}^6$, and $\underline{b}(t) \in \mathbb{R}^6, t \in [0,T]$, is the vector-valued function defined in (A3). In (22) and in the sequel we use the standard rows by columns matrix vector multiplication.

Problem (22) and (23) is the final value problem for a system of Riccati ordinary differential equations. Let us assume that the final value problem (22) and (23) has a solution defined for $t \in [0,T]$. If this is not the case assumption (21) must be abandoned and problem (16) and (12) cannot be solved with the elementary technique used here. Equations (13), (14), and (21) imply that the optimal control solution of Problem 1 is given by

$$f_1^*(t,x,v) = \frac{1}{w_2}(\varepsilon(t) + 2\varphi(t)x + \delta(t)v) + \mu, \quad t \in [0,T], \ x \in \mathbb{R}, \ v \in \mathbb{R}_\epsilon, \tag{24}$$

$$f_2^*(t,x,v) = \frac{1}{w_3}(\beta(t) + 2\gamma(t)v + \delta(t)x) + k(\theta - v), \quad t \in [0,T], \ x \in \mathbb{R}, \ v \in \mathbb{R}_\epsilon, \tag{25}$$

where in (24) and (25) the functions $\beta(t), \gamma(t), \delta(t), \epsilon(t), \varphi(t), t \in [0,T]$, are, respectively, the last five components of the vector-valued function $\underline{h}(t) = [\alpha(t), \beta(t), \gamma(t), \delta(t), \varepsilon(t), \varphi(t)]^\top, t \in [0,T]$, solution of (22) and (23).

Substituting the optimal control defined in (24) and (25) in (6) and (7), that is, choosing $f_1 = f_1^*, f_2 = f_2^*$, given by (24) and (25), in (6) and (7), we have

$$dx^*(t) = \left(\tfrac{1}{w_2}(\varepsilon(t) + 2\varphi(t)x^*(t) + \delta(t)v^*(t)) + \mu - \tfrac{1}{2}v^*(t)\right)dt + \sqrt{v^*(t)}\,dB(t), \ t \in [0,T], \tag{26}$$

$$dv^*(t) = \left(\tfrac{1}{w_3}(\beta(t) + 2\gamma(t)v^*(t) + \delta(t)x^*(t)) + k(\theta - v^*(t))\right)dt + \sigma\sqrt{v^*(t)}\,dZ(t), t \in [0,T], \tag{27}$$

with the initial conditions

$$x^*(0) = 0, \tag{28}$$

$$v^*(0) = v_0. \tag{29}$$

Model (26), (27), (28), (29), and (5) must be completed with the reflecting condition imposed on $v^* = \epsilon$ explained in Section 3. As already mentioned, Equation (5), originally formulated for Model 1, must be reinterpreted, before being added to Equations (26), (27), (28), and (29), to take care of the change of dependent variable made and of the choice of the control variables. Model (26), (27), (28), (29), and (5) (with the reflecting condition imposed) is the model resulting from the calibration in the real world of Model 2 and its transition probability density function is the density of the real

world probability measure associated with the data and the priors used in the calibration. It is easy to adapt the previous analysis to the situation where the reflecting condition $v^* = \epsilon$ is not necessary and is not imposed.

Unfortunately, the solution of problem (22) and (23), in general, is not expressed by a formula involving only "simple functions" even when $\tilde{x}(t)$, $t \in [0, T]$, is a simple function. Here, we refer to "simple functions" as functions expressed by elementary functions and by higher transcendental functions of common use, for example, the error function and its integral function. In the absence of an explicit solution, the final value problem (22) and (23) can be solved numerically, or using a perturbation method. We prefer to express the solution of (22) and (23) with a perturbation series. In fact, truncating this perturbation series, a closed form approximate solution of problem (22) and (23) involving only simple functions is obtained. This approximated solution can be easily evaluated numerically, eventually, taking advantage of parallel computing and/or of dedicated hardware architectures. In several practical circumstances, for example, when a quick response to unexpected changing situations makes a difference, the use of easy to evaluate closed form approximate solutions is preferable to the use of (accurate and computationally expensive) numerical solutions. This perturbation series is built introducing in problem (22) and (23) the auxiliary parameter p, $p \in [0, 1]$. That is, instead of (22) and (23), let us consider problem

$$\frac{d\underline{H}(t,p)}{dt} = D_p\underline{H}(t,p) + E_p(\underline{H}(t,p))\underline{H}(t,p) + \underline{b}(t), \quad t \in [0,T], \quad 0 \le p \le 1, \tag{30}$$

$$\underline{H}(T,p) = w_4\left[-\frac{1}{2}x_T^2, 0, 0, 0, x_T, -\frac{1}{2}\right]^\top, \quad 0 \le p \le 1, \tag{31}$$

where $\underline{H}(t,p) \in \mathbb{R}^6$, $t \in [0,T]$, $p \in [0,1]$, is a vector-valued function, D_p, $E_p(\underline{k})$, are 6×6 matrices defined in (A4) and (A5), $\underline{k} \in \mathbb{R}^6$, $p \in [0,1]$. Note that in (30), when $p = 0$, the first two equations are decoupled from the last four equations. This makes easy the solution of problem (30) and (23) when $p = 0$. Moreover, it is easy to see that when $p = 1$ the final value problem (30) and (31) coincides with the original final value problem (22) and (23). The auxiliary parameter p, $p \in [0,1]$, may be introduced in (22) and (23) in many different ways. This leads to different perturbation series. The choice made in (A4) and (A5) is only illustrative.

Let us assume that $\underline{H}(t,p)$, $t \in [0,T]$, $0 \le p \le 1$, solution of (30) and (31), can be written as a power series in p, that is, let us assume that

$$\underline{H}(t,p) = \underline{h}_0(t) + p\underline{h}_1(t) + p^2\underline{h}_2(t) + \cdots, \quad t \in [0,T], \quad 0 \le p \le 1, \tag{32}$$

where $\underline{h}_i(t) = [\alpha_i(t), \beta_i(t), \gamma_i(t), \delta_i(t), \varepsilon_i(t), \varphi_i(t)]^\top \in \mathbb{R}^6$, $t \in [0,T]$, $i = 0, 1, ...,$ are vector-valued functions to be determined. Substituting (32) in (30) and (23) and using the polynomial identity principle we determine the final value problems satisfied by the vector-valued functions $\underline{h}_i(t)$, $t \in [0,T]$, $i = 0, 1, ...$ We have (i) at zeroth order in p:

$$\frac{d\underline{h}_0(t)}{dt} = D_0\underline{h}_0(t) + E_0(\underline{h}_0(t))\underline{h}_0(t) + \underline{b}(t), \quad t \in [0,T], \tag{33}$$

$$\underline{h}_0(T) = w_4\left[-\frac{1}{2}x_T^2, 0, 0, 0, x_T, -\frac{1}{2}\right]^\top, \tag{34}$$

where D_0, $E_0(\underline{k})$ are 6×6 matrices defined in (A6) and (A7), $\underline{k} \in \mathbb{R}^6$.

The solution of the final value problem (33) and (34) is expressed by a formula involving only simple functions that has been obtained with the help of symbolic computation. That is, it has been obtained with the help of MATLAB Symbolic Math Toolbox. The possibility of finding a formula expressed in terms of simple functions for $\underline{h}_0(t)$, $t \in [0,T]$, depends on the fact that in Section 3 the function $\tilde{x}(t)$, $t \in [0,T]$, is chosen as a polynomial in $t^{1/2}$. More general choices of $\tilde{x}(t)$, $t \in [0,T]$, may lead to formulae involving quadratures of $\tilde{x}(t)$, $t \in [0,T]$, that cannot be expressed by simple functions, these quadratures can be eventually approximated by simple functions or can be evaluated numerically. For simplicity, the formula of the solution of (33) and (34) is omitted, (ii) at first order in p:

$$\frac{d\underline{h}_1(t)}{dt} = F_1(\underline{h}_0(t))\underline{h}_1(t) + \underline{b}_1(\underline{h}_0(t)), \quad t \in [0,T], \tag{35}$$

$$\underline{h}_1(T) = [0, 0, 0, 0, 0, 0]^\top, \tag{36}$$

where $F_1(\underline{k})$ is a 6×6 matrix, $\underline{b}_1(\underline{k}) \in \mathbb{R}^6$ are given by (A8) and (A9), $\underline{k} \in \mathbb{R}^6$.

With the choice of $\tilde{x}(t)$, $t \in [0, T]$, made in Section 3 (i.e., a polynomial of degree 2 in the variable $t^{1/2}$), with the exception of $\beta_1(t)$, $t \in [0, T]$, the solution of the final value problem (35) and (36) is expressed by a formula involving only simple functions that has been obtained with the help of symbolic computation. That is, it has been obtained with the help of MATLAB Symbolic Math Toolbox. The function $\beta_1(t)$, $t \in [0, T]$, is expressed as a power series in $t^{1/2}$ and is approximated with a polynomial in $t^{1/2}$ truncating the power series. For simplicity the formula of the solution of (35) and (36) is omitted.

The function $\underline{h}(t)$, $t \in [0, T]$, solution of (22) and (23) is approximated with the power series in p (32) of $\underline{h}(t, p)$, $t \in [0, T]$, $0 \le p \le 1$, truncated at first order in p and evaluated in $p = 1$, that is, $\underline{h}(t)$, $t \in [0, T]$, solution of (22) and (23), is approximated with $\hat{\underline{h}}(t)$, $t \in [0, T]$, where

$$\hat{\underline{h}}(t) = \underline{h}_0(t) + \underline{h}_1(t), \quad t \in [0, T]. \tag{37}$$

Substituting (37) in (24) and (25) we have an approximated optimal control of Problem 1 expressed by a formula involving only simple functions. The approximated optimal control formula deduced from (37), (21), (13), and (14) can be easily evaluated and used in practical circumstances.

To the approximated optimal control, found as consequence of (37), corresponds the dynamics of the asset log returns and of the stochastic variance defined by the following system of stochastic differential equations:

$$\begin{aligned} d\hat{x}^*(t) = &\left(\frac{1}{w_2}(\hat{\epsilon}(t) + 2\hat{\varphi}(t)\hat{x}^*(t) + \hat{\delta}(t)\hat{v}^*(t)) + \mu - \frac{1}{2}\hat{v}^*(t)\right)dt \\ &+ \sqrt{\hat{v}^*(t)}\, dB(t), \, t \in [0, T], \end{aligned} \tag{38}$$

$$\begin{aligned} d\hat{v}^*(t) = &\left(\frac{1}{w_3}(\hat{\beta}(t) + 2\hat{\gamma}(t)\hat{v}^*(t) + \hat{\delta}(t)\hat{x}^*(t)) + k(\theta - \hat{v}^*(t))\right)dt \\ &+ \sigma\sqrt{\hat{v}^*(t)}\, dZ(t), \, t \in [0, T], \end{aligned} \tag{39}$$

with the initial conditions

$$\hat{x}^*(0) = 0, \tag{40}$$

$$\hat{v}^*(0) = v_0, \tag{41}$$

where in (38) and (39) we have $\hat{\beta}(t) = \beta_0(t) + \beta_1(t)$, $\hat{\gamma}(t) = \gamma_0(t) + \gamma_1(t)$, $\hat{\delta}(t) = \delta_0(t) + \delta_1(t)$, $\hat{\epsilon}(t) = \epsilon_0(t) + \epsilon_1(t)$, $\hat{\varphi}(t) = \varphi_0(t) + \varphi_1(t)$, $t \in [0, T]$ and (5). To the model (38), (39), (40), (41), and (5) must be added the reflecting condition imposed on the set $\{[\hat{x}^*, \hat{v}^*]^\top \in \mathbb{R}^2 \mid \hat{v}^* = \epsilon\}$. The stochastic processes $\hat{x}^*(t), \hat{v}^*(t)$, $t \in [0, T]$, solution of (38), (39), (40), (41), and (5) (with the reflecting condition imposed in $\hat{v}^* = \epsilon$) are the approximations of $x^*(t), v^*(t)$, $t \in [0, T]$, solution of (26), (27), (28), (29), and (5) (with the reflecting condition imposed) corresponding to the approximate solution obtained from the power series in p of $\underline{H}(t, p)$, $t \in [0, T]$, $0 \le p \le 1$, truncated at the first order and evaluated in $p = 1$. The transition probability density function of (38), (39), (40), (41), and (5), with the reflecting boundary condition imposed on the set $\{[\hat{x}^*, \hat{v}^*]^\top \in \mathbb{R}^2 \mid \hat{v}^* = \epsilon\}$, is the approximated probability density function of the real world probability measure $\mathbb{P}$, associated with the time series of asset log returns used as data, and to the priors chosen in the formulation of the optimal control problem, obtained from the approximated solution of Problem 1 (with the reflecting condition imposed).

3 | NUMERICAL EXPERIMENTS

First of all, let us explain the reflecting condition, announced in Section 2, imposed on the paths of the stochastic processes $x(t), v(t)$, $t \in [0, T]$. We proceed as done in Ladd and Szymczak (2003). Let $\epsilon > 0$ be given, $\mathbb{R}^2_\epsilon = \{[x, v]^\top \in \mathbb{R}^2 \mid v > \epsilon\}$, $\partial\mathbb{R}^2_\epsilon = \{[x, \epsilon]^\top \in \mathbb{R}^2 \mid x \in \mathbb{R}\}$ be the boundary of $\mathbb{R}^2_\epsilon$, $\underline{n} = \underline{n}([x, \epsilon]^\top) = [0, -1]^\top \in \mathbb{R}^2$, be the outward unit normal vector of the domain $\mathbb{R}^2_\epsilon$ in the point $[x, \epsilon]^\top \in \partial\mathbb{R}^2_\epsilon$, $x \in \mathbb{R}$, and $\forall\ \underline{a}, \underline{b} \in \mathbb{R}^2$ let $\underline{a} \cdot \underline{b}$ be the

Euclidean scalar product in $\mathbb{R}^2$ of $\underline{a}$ and $\underline{b}$. For simplicity, to avoid the mathematical subtleties mentioned in Section 1, the reflecting condition is imposed (when necessary) in $v = \epsilon$ instead of being imposed in $v = 0$ (as it should be). When $\tau \in (0, T)$ is such that $v(\tau^-) = \epsilon$ and $[dx(\tau^-), dv(\tau^-)]^\top \cdot \underline{n} > 0$, the reflecting condition imposed is

$$[dx(\tau^+), dv(\tau^+)]^\top \cdot \underline{n} = -[dx(\tau^-), dv(\tau^-)]^\top \cdot \underline{n}\,, \quad \tau \in (0, T), \tag{42}$$

where $dx(\tau^+), dv(\tau^+), dx(\tau^-), dv(\tau^-)$ are, respectively, the right and left limit of $dx(t), dv(t), t \in (0, T)$, when $\tau \in (0, T)$ and t goes to τ. Similarly $x(\tau^+), v(\tau^+), x(\tau^-), v(\tau^-)$ denote, respectively, the right end left limit of $x(t), v(t), t \in [0, T]$, when $\tau \in (0, T)$ and t goes to τ. Equation (42) is a condition imposed on the normal component to $\partial\mathbb{R}^2_\epsilon$ of the vector $[dx(\tau^+), dv(\tau^+)]^\top$ given the normal component to $\partial\mathbb{R}^2_\epsilon$ of the vector $[dx(\tau^-), dv(\tau^-)]^\top$. When $\tau \in (0, T)$, $v(\tau^-) = \epsilon$ and $[dx(\tau^-), dv(\tau^-)]^\top \cdot \underline{n} > 0$, $\underline{n} = [0, -1]^\top$, the reflecting condition (42) becomes $dv(\tau^+) = -dv(\tau^-)$. Together with (42), it is imposed the continuity in $t = \tau$ of the tangential component to $\partial\mathbb{R}^2_\epsilon$ of the vector $[dx(t), dv(t)]^\top$, and of the paths of the stochastic processes $x(t), v(t), t \in [0, T]$, that is, it is imposed $dx(\tau^+) = dx(\tau^-)$ and $x(\tau^+) = x(\tau^-), v(\tau^+) = v(\tau^-)$. The previous conditions define $dx(\tau^+), dv(\tau^+), x(\tau^+), v(\tau^+)$ given $dx(\tau^-), dv(\tau^-), x(\tau^-), v(\tau^-)$. When Model 1 is considered, similar conditions are imposed on the paths of the stochastic processes $S(t), v(t), t \in [0, T]$.

As already mentioned, the reflecting condition imposed on the oc model plays the same role as the Feller condition in the Heston model and guarantees the positivity of the stochastic variance and the probabilistic interpretation of the model. However, in the numerical experiments presented rarely the reflecting condition is active. In fact, only 0.01% of the trajectories of the stochastic variance computed in the numerical experiments hits zero and "activates" the reflecting condition. Now, let us introduce the data sets studied in the numerical experiments. The real data consists of the time series of the daily closing values of the S&P500 index of the NYSE in the period January 2, 2009–January 4, 2018. To generate the synthetic data, first of all the Heston model is calibrated using the real data mentioned above. The synthetic data are the time series of the daily asset prices obtained simulating one trajectory of the calibrated Heston model. This trajectory is computed by integrating numerically, with the explicit Euler finite difference scheme (Andersen, 2008), an initial value problem for the calibrated Heston model. The initial stochastic variance of this trajectory comes from the calibration of the Heston model while the initial asset price is taken from the S&P500 data (i.e., it is the closing S&P500 index value of January 2, 2009). The synthetic asset prices and log returns, obtained in this way, are called, respectively, Heston model prices and Heston model log returns. For simplicity and ease of comparison with real data experiments, the simulated Heston model trajectory is associated with the time period January 2, 2009–January 4, 2018. In the numerical experiments the unit on the time axis corresponds to one "year", 1 year is made of 12 months, and 1 month is made of 21 (consecutive) trading days. This means that 1 year is made of 12 (months) $\times$21 (trading days/month) = 252 trading days. In fact, there are approximately 252 days of open markets in a calendar year. Note that the days of closed markets are removed from the time axis and that on the time axis 1 trading day corresponds to an interval of length $\Psi = 1/252$ years. In particular, the month of the forecasts is a month made of 21 consecutive trading days. For later convenience, let us note that 30 months = 30 (months) $\times$21 (trading days/month) = 630 trading days. The Heston and the oc models are calibrated using, respectively, daily returns and monthly log returns of the S&P500 index associated with the daily closing values of the S&P500 index relative to a time period of 30 (consecutive) months together with three priors. Given a set of daily return data relative to a period of 30 (consecutive) months, we begin calibrating the Heston model. The calibrated Heston model provides the numerical values of the parameters $\mu, k, \theta, v_0, \rho, \sigma$ defined in Section 2, which appear in the priors and in Problem 1, that are used to calibrate the oc model with the monthly log return data relative to the same 30 months period used to calibrate the Heston model. The prior x_T of (9) is chosen with a fitting procedure based on the log return data used in the oc model calibration that is explained later. The Heston and the oc models are calibrated once a month across a period of, respectively, 72, 66, and 55 months when 6, 12, and 24 months in the future forecasts are produced, that is, they are calibrated, respectively, 72, 66, and 55 times when 6, 12, and 24 months in the future forecasts are produced. The calibration problems relative to different months use different windows of 30 (consecutive) months of data. Let $H > 0$ a positive integer, for $h = 1, 2, ..., H$, let $t^h = 630/252\text{years} + (h-1)\Delta_1$, where $\Delta_1 = 21/252$ years = 1 month, be the time corresponding to the (beginning of) the first trading day of the hth month, that follows a window of 630 consecutive daily observations of the S&P500 index (or the Heston model price) extracted from the data sets previously specified. Note that when $h = 1$ we choose $t = 0$ years corresponding to January 2, 2009 and that $t^{h+1} - t^h = \Delta_1 = 1$ month, $h = 1, 2, ..., H-1$.

Moreover, let us point out that, since we have defined a month as made of 21 consecutive trading days, the first day of a month, in the sense used here, may not coincide with the first day of a month in the calendar sense. To compare the 6, 12, and 24 months forecasts, it is necessary that the forecasting times of the different forecasts coincide. For this reason, we have chosen, respectively, $H = 72, 66$, and 55 when 6, 12, and 24 months in the future forecasts are produced. In the rest of the paper we have $H = 72$ or 66 or 55 depending on the forecasts considered.

Let us explain the method used to calibrate the Heston model in the hth calibration problem, that is, in the problem associated with the month that begins at time t^h, $h = 1, 2, ..., H$. That is, for example, is the hth problem 6 months in the future forecast means the log return forecast 6 months after time $t = t^h$, $h = 1, 2, ..., H$. For $h = 1, 2, ..., H$ in the hth calibration problem the time t^h is the current time, that is, the observations end at time t^h and the time values greater than t^h are in the future. In the hth calibration problem the Heston model is calibrated using as data the daily closing values of the S & P500 index (or the Heston model daily prices) and the corresponding S & P500 index daily returns (or the Heston model daily returns) associated with the 30 consecutive months of data that end at time t^h, $h = 1, 2, ..., H$. That is, let $N = 630$ and $S_1, S_2, ..., S_N$ be the daily closing values of the S&P500 index observed (or the Heston model daily prices), respectively, at times $\tau_1, \tau_2, ..., \tau_N$, where $\tau_i = t^h - \Psi(N - i)$, $i = 1, 2, ..., N$, the S&P500 index daily return (or the Heston model daily return) r_i at time τ_i is the return of the S&P500 index (or the Heston model daily return) at time τ_{i+1} with respect to the S&P500 index (or the Heston model price) at time τ_i, this is, $r_i = \frac{S_{i+1} - S_i}{S_i}$, $i = 1, 2, ..., N - 1$. Note that to keep the notation simple (for all the values of i considered) the dependence of τ_i, S_i, r_i from h is omitted, $h = 1, 2, ..., H$. For $h = 1, 2, ..., H$ the hth calibration problem for the Heston model is solved using the data set associated with time t^h. That is, for $h = 1, 2, ..., H$ the Heston model parameters $\mu, k, \theta, v_0, \rho, \sigma$, defined in Section 2, are estimated using the data window associated with time t^h. Let $\hat{\mu}, \hat{k}, \hat{\theta}, \hat{v}_0, \hat{\rho}, \hat{\sigma}$ be, respectively, the estimates of $\mu, k, \theta, v_0, \rho, \sigma$, obtained at time t^h, $h = 1, 2, ..., H$. For simplicity the dependence of these estimates from the data window considered, that is, their dependence from h, is omitted, $h = 1, 2, ..., H$. The drift rate of the asset price equation of the Heston model μ is estimated as the mean drift rate deduced from the observed S&P500 index daily returns (or the Heston model daily returns), that is, we have

$$\hat{\mu} = \frac{1}{\Psi}\left(\frac{1}{N-1}\sum_{i=1}^{N-1} r_i\right). \tag{43}$$

To estimate the parameters k, θ, σ of the stochastic variance equation of the Heston model and the initial stochastic variance v_0, we use as "data" the 20 days running daily realized variance of the S&P500 index returns (or the Heston model returns) and of the corresponding "observation times" associated with the data window specified above. That is, we consider the realized variance:

$$\hat{v}_i = \frac{1}{\Psi}\left(\frac{1}{19}\sum_{j=i-20+1}^{i} (r_j - \Psi\hat{\mu}_i)^2\right) \quad \text{as "observed" at time } \tau_i, \quad i = 20, 21, ..., N - 1, \tag{44}$$

where $\hat{\mu}_i = \frac{1}{\Psi}\left(\frac{1}{20}\sum_{j=i-20+1}^{i} r_j\right)$, $i = 20, 21, ..., N - 1$. The quantities defined in (44) are a sample of $N - 20 = 610$ 20 days running realized variances and of the corresponding "observation times." In the sequel the "data" defined in (44) are used as a time series of "observations" of the (unobservable) stochastic variance of the Heston model. The estimate $\hat{v}_0$ of the initial stochastic variance v_0 is simply $\hat{v}_{20}$, that is, we have $\hat{v}_0 = \hat{v}_{20}$. The parameters k, θ, σ of the stochastic variance equation of the Heston model are estimated using the martingale estimation approach (Bibby & Sørensen, 1995; Kloeden & Platen, 1992) and the "data" time series defined in (44). That is, let us consider the stochastic differential equation

$$dv(t) = (a + bv(t))dt + \sigma\sqrt{v(t)}\,dZ(t), \quad t \in [0, T], \tag{45}$$

where a, b, σ are real constants and $dZ(t)$, $t \in [0, T]$, is the stochastic differential of a Wiener process $Z(t)$, $t \in [0, T]$, such that $Z(0) = 0$. Later in (45) we choose $b = -k$ and $a = k\,\theta$. Note that when $b = -k$ and $a = k\theta$ Equation (45)

coincides with Equation (2) when $\tilde{f}_2(t,S,v) = k(\theta - v), t \in [0,T], S, v \in \mathbb{R}_+$, and that Equation (2) when $\tilde{f}_2(t,S,v) = k(\theta - v), t \in [0,T], S, v \in \mathbb{R}_+$, is the stochastic variance equation of the Heston model. The conditions $k, \theta \in \mathbb{R}_+, \sigma \neq 0, \frac{2k\theta}{\sigma^2} > 1$, that are imposed on the parameters of the stochastic variance equation of the Heston model, are easily translated in conditions on the parameters a, b, σ of (45) using the relations $b = -k, a = k\,\theta$. Note that the parameter σ remains unaltered going from Equation (45) to the same equation rewritten in the notation used for the stochastic variance equation of the Heston model. The martingale estimation method, see Bibby and Sørensen (1995) and Kloeden and Platen (1992), finds the estimates of the parameters a, b, σ discretizing (45) with the strong Taylor scheme, obtained by adding to the Milstein scheme extra terms taken from the Itô–Taylor expansion of (45). That is, starting from $\hat{v}_{20}, \hat{v}_{21}, ..., \hat{v}_{N-1}$, defined in (44), considered as a sequence of "observations" of the solution of (45), made, respectively, at the "observation times" $\tau_{20}, \tau_{21}, ..., \tau_{N-1}$, we find the estimates $\hat{b}, \hat{a}, \hat{\sigma}$ of the parameters b, a, σ of (45) that follow:

$$\hat{b} = \frac{1}{\Psi} \ln \left(\frac{(N-20)\sum_{i=21}^{N} \frac{\hat{v}_i}{\hat{v}_{i-1}} - \left(\sum_{i=21}^{N} \hat{v}_i\right)\left(\sum_{i=21}^{N} \frac{1}{\hat{v}_{i-1}}\right)}{(N-20)^2 - \left(\sum_{i=21}^{N} \hat{v}_{i-1}\right)\left(\sum_{i=21}^{N} \frac{1}{\hat{v}_{i-1}}\right)} \right), \tag{46}$$

$$\hat{a} = \frac{\hat{b}}{1 - e^{\hat{b}\Psi}} \frac{(N-20)e^{\hat{b}\Psi} - \sum_{i=21}^{N} \frac{\hat{v}_i}{\hat{v}_{i-1}}}{\sum_{i=21}^{N} \frac{1}{\hat{v}_{i-1}}}, \tag{47}$$

$$\hat{\sigma} = \left(\frac{\sum_{i=21}^{N} \left(\hat{v}_i - \frac{(\hat{a} + \hat{b}\hat{v}_{i-1})e^{\hat{b}\Psi} - \hat{a}}{\hat{b}} \right)^2 \frac{1}{\hat{v}_{i-1}}}{\sum_{i=21}^{N} \left(\frac{(\hat{a} + 2\hat{b}\hat{v}_{i-1})e^{2\hat{b}\Psi} - 2(\hat{a} + \hat{b}\hat{v}_{i-1})e^{\hat{b}\Psi} + \hat{a}}{2\hat{v}_{i-1}\hat{b}^2} \right)} \right)^{1/2}. \tag{48}$$

When $b = -k, a = k\,\theta$ from (46) and (47), it is easy to find the estimates $\hat{k}, \hat{\theta}$ of, respectively, the parameters k, θ of the stochastic variance equation of the Heston model, in fact, we have $\hat{k} = -\hat{b}, \hat{\theta} = -\hat{a}\,/\hat{b}$. The estimate $\hat{\sigma}$ of σ, given in (48), remains unaltered when Equation (45) is rewritten in the notation used for the stochastic variance equation of the Heston model. Finally, the estimate $\hat{\rho}$ of the correlation coefficient ρ of (5) is given by the sample correlation between the time series $r_{20}, r_{21}..., r_{N-1}$ and $\hat{v}_{20}, \hat{v}_{21}, ... \hat{v}_{N-1}$, that is,

$$\hat{\rho} = \frac{(N-20)\sum_{i=20}^{N-1} r_i \hat{v}_i - \left(\sum_{i=20}^{N-1} r_i\right)\left(\sum_{i=20}^{N-1} \hat{v}_i\right)}{\sqrt{(N-20)\sum_{i=20}^{N-1} r_i^2 - \left(\sum_{i=20}^{N-1} r_i\right)^2}\sqrt{(N-10)\sum_{i=20}^{N-1} \hat{v}_i^2 - \left(\sum_{i=20}^{N-1} \hat{v}_i\right)^2}}. \tag{49}$$

When for some i we have $\hat{v}_i = 0$ or when we have $\hat{b} = 0$, the expressions (46), (47), and (48) and the expression of $\hat{\theta} = \frac{\hat{a}}{\hat{b}}$ contain divisions by zero and have no meaning. Moreover, the previous estimates $\hat{\theta}, \hat{k}, \hat{\sigma}$ must satisfy the conditions $\hat{\theta}, \hat{k} \in \mathbb{R}_+, \hat{\sigma} \neq 0, \frac{2\hat{k}\,\hat{\theta}}{\hat{\sigma}^2} > 1$ to guarantee that Equation (45), resulting from the calibration, is a legitimate stochastic variance equation. For this reason, given $\eta > 0$, when: for some i we have $\hat{v}_i < \epsilon, \hat{a} < \eta, |\hat{\sigma}| < \eta, \hat{b} > -\eta$ we replace $\hat{v}_i, \hat{a}, \hat{\sigma}, \hat{b}$ with, respectively, $\epsilon, \eta, \eta, -\eta$. The fact that the reflecting condition (42) is imposed in $v = \epsilon$ justifies the choice of replacing $\hat{v}_i$ with ϵ when $\hat{v}_i < \epsilon, i = 20, 21, ..., N-1$. The quantity η is simply a threshold value used to avoid numerical troubles, that guarantees that Equation (45) can be interpreted as a legitimate stochastic variance equation. In the calibration problems considered, when the condition $\frac{2\hat{k}\,\hat{\theta}}{\hat{\sigma}^2} > 1$ is not satisfied, it is enforced considering Equations (47) and (48) not as equalities but in the constrained least-squares sense. That is, to the least-squares formulation of (47) and (48) are added the constraints that express the required conditions. The solution of the resulting constrained least-squares problem defines the estimates $\hat{a}, \hat{\sigma}$ of a, σ. The estimates $\hat{\mu}, \hat{k}, \hat{\theta}, \hat{v}_0, \hat{\rho}, \hat{\sigma}$ of $\mu, k, \theta, v_0, \rho, \sigma$, defined above, are the values of the parameters of the Heston model, obtained as solution of the calibration problem formulated at time $t^h, h = 1, 2, ..., H$.

Now, let us calibrate the oc model at time t^h, that is, let us explain how Problem 1 is formulated and solved in the hth calibration problem, $h = 1, 2, ..., H$. First of all, for $h = 1, 2, ..., H$, the estimates $\hat{\mu}, \hat{k}, \hat{\theta}, \hat{v}_0, \hat{\rho}, \hat{\sigma}$ of the parameters of the Heston model, calibrated at time t^h, are chosen as values, respectively, of the parameters $\mu, k, \theta, v_0, \rho, \sigma$ of the calibration problem at time t^h of the oc model, that is of Problem 1. Moreover, in the hth oc model calibration problem let us choose $T_1 = t^h$ years, $h = 1, 2, ..., H$. With the previous choice of T_1, the time $t = 0$ years of the hth calibration problem corresponds to the first observation day of the data window used to calibrate the oc model at time t^h, $h = 1, 2, ..., H$. We consider as data of the oc model calibration problem the asset log returns with respect to the asset price at time $t = 0$ years observed at the end of each month in the time period of 30 (consecutive) months that ends at time t^h, that is, we consider the log returns $\tilde{x}_i$, $i = 1, 2, ..., m$, observed, respectively, at the times $t_i = t^h - \Delta_1(m - i)$, $i = 1, 2, ..., m$, where $m = 30$. In the study of the oc model calibration problems two time scales are used, the first scale is the scale associated with the physical time (i.e., the "calendar scale" that is obtained by removing from the calendar the days of closed market, this is the scale used in Figures 1–3), the second scale depends on the calibration problem considered and in the hth month calibration problem is associated with the choice $T_1 = t^h$ years, $h = 1, 2, ..., H$. Note that these scales are transformed one in the other by suitable translations of the time axis. Occasionally we switch from one scale to a second scale and it is left to the reader to understand when these switches occur. The weights w_i, $i = 1, 2, ..., 4$, of the functional (9) are chosen (with a trial and error procedure) to guarantee that the expected value of the four addenda of (9) (in absolute value) at the optimizer of Problem 1 is of the same order of magnitude. The weights w_i, $i = 1, 2, ..., 4$, of the hth calibration problem depend (in general) on h. However, to simplify the notation, this dependence is omitted, $h = 1, 2, ..., H$.

In the numerical experiments involving real data the following three cases are studied: $T_1 = T - 6\Delta_1$, $T_1 = T - 12\Delta_1$, $T - T_1 = 24\Delta_1$, this corresponds, respectively, to the 6, 12, and 24 months in the future forecasting experiment of the S&P500 index discussed below. For simplicity, in the numerical experiments involving synthetic data only the case $T_1 = T - 6\Delta_1$ is studied, that is, only the 6 months in the future forecasting experiment is considered.

When $T - T_1 = 6\Delta_1$ the function $\tilde{x}(t)$, $t \in [0, T]$, of (9) is chosen as the polynomial $q(t)$, $t \in [0, T]$, of degree three in the variable $t^{1/2}$ that fits in the weighted least-squares sense the m points $(t_i, \tilde{x}_i)$, $i = 1, 2, ..., m$, $m = 30$, that is, $\tilde{x}(t) = q(t) = q_{6\Delta_1}(t)$, $t \in [0, T]$. The prior x_T of (9) is chosen as $x_T = \tilde{x}(T) = q(T) = q_{6\Delta_1}(T)$. In the weighted least-squares procedure used to determine $\tilde{x}(t)$, $t \in [0, T]$, the residuals of the more recent observations have bigger weights than the residuals of the observations deeper in the past. More precisely, we assign the weight $\frac{2i}{m(m+1)}$ to the residual associated with the observation $(t_i, \tilde{x}_i)$, where $t_i = T_1 + (i - m)\Delta_1$, $i = 1, 2, ..., m$, $m = 30$. When $T - T_1 = 6\Delta_1$ Problem 1, formulated as specified above, is solved with the procedure suggested in Section 2. Using the calibrated oc model,

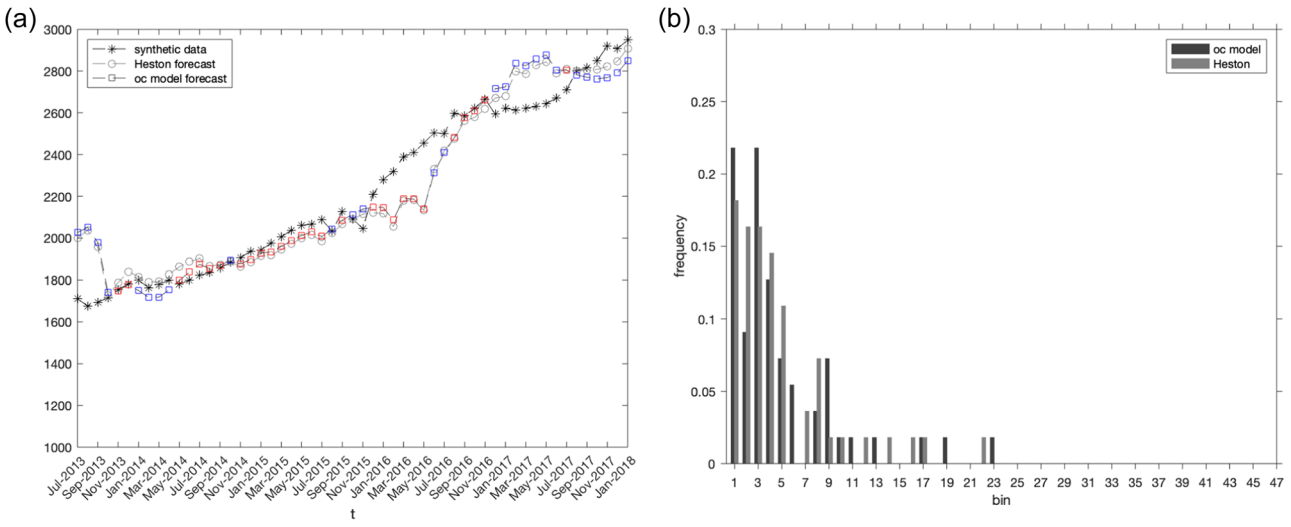

FIGURE 1 (a) Trajectory of the simulated Heston model price (-*-) and the corresponding trajectories of the forecasted price 6 months in the future with the oc (-□-) and the Heston (-○-) models. (b) Frequency histogram of the relative errors committed approximating the simulated Heston model price with the forecasted price 6 months in the future with the oc (in the dark gray) and the Heston (in light gray) models.

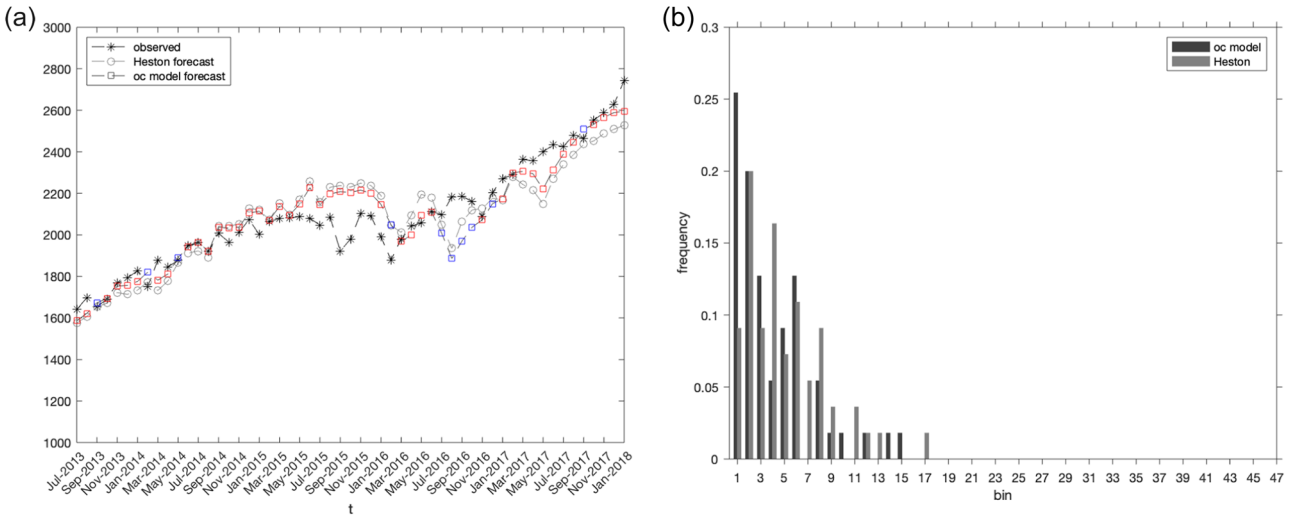

FIGURE 2 (a) Trajectory of the observed S&P500 index (-*-) and the corresponding trajectories of the forecasted S&P500 index 6 months in the future with the oc (-□-) and the Heston (-○-) models. (b) Frequency histogram of the relative errors committed approximating the observed S&P500 index with the forecasted S&P500 index 6 months in the future with the oc (in the dark gray) and the Heston (in light gray) models.

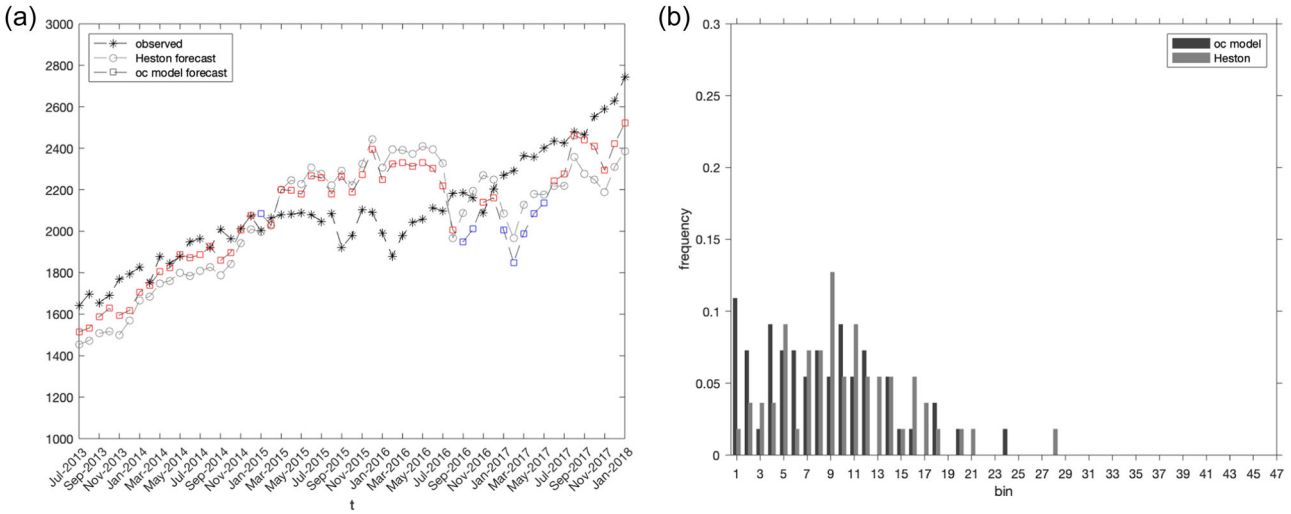

FIGURE 3 (a) Trajectory of the observed S&P500 index (-*-) and the corresponding trajectories of the forecasted S&P500 index 12 months in the future with the oc (-□-) and the Heston (-○-) models. (b) Frequency histogram of the relative errors committed approximating the observed S&P500 index with the forecasted S&P500 index 12 months in the future with the oc (in the dark gray) and the Heston (in light gray) models.

monthly forecasted asset log returns up to 6 months in the future, that is, up to 6 months after $t = T_1$, are computed. The forecasted asset log return at a given forecasting time, obtained with the Heston or with the oc model calibrated at time t^h, is the conditional expectation at the forecasting time of the stochastic process corresponding to the asset log returns, respectively, in the calibrated Heston or oc model at time t^h given the observation $\tilde{x}_m$ of the log return at time $t = t_m$. Recall that in the hth month calibration problem we have $T_1 = t^h = t_m$, $h = 1, 2, ..., H$. Similarly, it is defined as the forecasted variance. As usual, for simplicity, the dependence from h of T_1 and t_m is omitted. In the numerical experiments the conditional expectations, needed to obtain the forecasts considered, are computed using statistical simulation. There are several other possibilities for defining the forecasts that are used in the numerical experiments. For simplicity we do not consider them here.

To obtain the oc model forecasted log returns up to 12 months in the future, $x^{oc}_{12\Delta_1}(t_i)$, $t_i = T_1 + (i-m)\Delta_1$, $i = 1, m+2, ..., m+12$, we solve Problem 1 two times, in two different time intervals: $[0, T_1 + 6\Delta_1]$ and $[0, T_1 + 12\Delta_1]$. Let $x^{oc}_{6\Delta_1}(t_i)$, $v^{oc}_{6\Delta_1}(t_i)$ be, respectively, the forecasted asset log returns and the forecasted stochastic variances at time $t_i = T_1 + (i-m)\Delta_1$, $i = m+1, m+2, ..., m+6$, obtained as solution of Problem 1 in the time interval $[0, T_1 + 6\Delta_1]$. We begin putting $x^{oc}_{12\Delta_1}(t_i) = x^{oc}_{6\Delta_1}(t_i)$, $t_i = T_1 + (i-m)\Delta_1$, $i = m+1, m+2, ..., m+6$, and we compute the polynomial $q_{12\Delta_1}(t)$, $t \in [0, T_1 + 12\Delta_1]$, of degree three in the variable $t^{1/2}$ that fits in the weighted least-squares sense the $m+6$ (where $m+6 = 36$) "observations" made of the m observed points $(t_i, \tilde{x}_i)$, $i = 1, 2, ..., m$, $m = 30$, and of the six forecasted points $\left(t_i, x^{oc}_{6\Delta_1}(t_i)\right)$, $i = m+1, m+2, ..., m+6$. The weights of the least-squares procedure, used to fit the $m+6$ "data" points mentioned above, are chosen in analogy with the choice of the weights done in the time interval $[0, T_1 + 6\Delta_1]$. Next, we solve Problem 1 in the time interval $[0, T_1 + 12\Delta_1]$ choosing $\tilde{x}(t) = q_{12\Delta_1}(t)$, $t \in [0, T]$, $x_T = q_{12\Delta_1}(T)$, $T = T_1 + 12\Delta_1$, and we compute the forecasted asset log returns in the time interval $[T_1 + 6\Delta_1, T_1 + 12\Delta_1]$, $x^{oc}_{12\Delta_1}(t_i)$, where $t_i = T_1 + (i-m)\Delta_1$, $i = m+6, m+7, ..., m+12$, as expected value of the suitable random variables obtained from the calibrated oc model trajectories obtained solving (6), (7), and (5) with the drift terms resulting from the calibration and the initial condition $x_0 = x^{oc}_{6\Delta_1}(t_{m+6})$, $v_0 = v^{oc}_{6\Delta_1}(t_{m+6})$.

In analogy with what it is done for the oc model, the Heston model forecasted log returns up to 12 months in the future, $x^{h}_{12\Delta_1}(t_i)$, $t_i = T_1 + (i-m)\Delta_1$, $i = m+1, m+2, ..., m+12$, are obtained calibrating the Heston model using as data the daily log returns of the S & P500 index associated with the 30 consecutive months of data that end at time $t = t_m = T_1$. Let $x^{h}_{6\Delta_1}(t_i)$, $v^{h}_{6\Delta_1}(t_i)$ be, respectively, the forecasted asset log returns and stochastic variances at time $t_i = T_1 + (i-m)\Delta_1$, $i = m+1, m+2, ..., m+6$, obtained with the calibrated Heston model in the time interval $[0, T_1 + 6\Delta_1]$. First of all we choose $x^{h}_{12\Delta_1}(t_i) = x^{h}_{6\Delta_1}(t_i)$, $i = m+1, m+2, ..., m+6$. Next, we compute the Heston model forecasted asset log returns in the time interval $[T_1 + 6\Delta_1, T_1 + 12\Delta_1]$, $x^{h}_{12\Delta_1}(t_i)$, where $t_i = T_1 + (i-m)\Delta_1$, $i = m+6, m+7, ..., m+12$, as expectation of the calibrated Heston model trajectories with initial conditions $x_0 = x^{h}_{6\Delta_1}(t_{m+6})$, $v_0 = v^{h}_{6\Delta_1}(t_{m+6})$.

To obtain the oc model forecasted log returns up to 24 months in the future, $x^{oc}_{24\Delta_1}(t_i)$, $t_i = T_1 + (i-m)\Delta_1$, $i = 1, m+2, ..., m+24$, we solve Problem 1 four times, in four different time intervals: $[0, T_1 + 6\Delta_1]$, $[0, T_1 + 12\Delta_1]$, $[0, T_1 + 18\Delta_1]$, and $[0, T_1 + 24\Delta_1]$. First of all we put $x^{oc}_{24\Delta_1}(t_i) = x^{oc}_{6\Delta_1}(t_i)$, $i = m+1, m+2, ..., m+6$, where $t_i = T_1 + (i-m)\Delta_1$, $i = m+1, m+2, ..., m+6$. In the remaining intervals (i.e., $[0, T_1 + 12\Delta_1]$, $[0, T_1 + 18\Delta_1]$, and $[0, T_1 + 24\Delta_1]$) we solve Problem 1 by choosing $T = T_1 + k\Delta_1$, $x_T = q_{k\Delta_1}(T)$ and $\tilde{x}(t) = q_{k\Delta_1}(t)$, $t \in [0, T_1 + k\Delta_1]$, $k = 12, 18, 24$, where $q_k(t)$ is the polynomial of degree three in the variable $t^{1/2}$ that fits in the weighted least-squares sense the $m+k-6$ "observations" made of the m observed points $(t_i, \tilde{x}_i)$, $i = 1, 2, ..., m$, $m = 30$, and of the $k-6$ forecasted points $\left(t_i, x^{oc}_{(k-6)\Delta_1}(t_i)\right)$, $i = m+1, m+2, ..., m+(k-6)$. The weights of the least-squares procedure, used to fit the $m+k-6$ "data" points considered, are chosen in analogy with the choice of the weights done in the time interval $[0, T_1 + 6\Delta_1]$. The $k-6$ forecasted values $x^{oc}_{(k-6)\Delta_1}(t_i)$, $i = m+1, m+2, ..., m+(k-6)$, are computed as expectation of the calibrated oc model trajectories obtained solving (6), (7), and (5) with the drift terms resulting from the calibration and the initial condition $x_0 = x^{oc}_{(k-12)\Delta_1}(t_{m+k-12})$, $v_0 = v^{oc}_{(k-12)\Delta_1}(t_{m+k-12})$, $k = 12, 18, 24$. The 24 months in the future forecasted log returns after the original choice $t = T_1$ are given by $x^{oc}_{24\Delta_1}(t_i) = x^{oc}_{k\Delta_1}(t_i)$, $i = m+k-6, m+2, ..., m+k$, $k = 12, 18, 24$.

In analogy with what it is done for the oc model, the Heston model forecasted log returns up to 24 months in the future, $x^{h}_{24\Delta_1}(t_i)$, $t_i = T_1 + (i-m)\Delta_1$, $i = 1, m+2, ..., m+24$, are obtained calibrating the Heston model once using as data the daily log returns of the S & P500 index, associated with the 30 consecutive months of data that end at time $t = t_m = T_1$. Next, we forecast the calibrated Heston model asset log returns in the time intervals: $[T_1, T_1 + 6\Delta_1]$, $[T_1 + 6\Delta_1, T_1 + 12\Delta_1]$, $[T_1 + 12\Delta_1, T_1 + 18\Delta_1]$, $[T_1 + 18\Delta_1, T_1 + 24\Delta_1]$. This is done as follows: first of all we put $x^{h}_{24\Delta_1}(t_i) = x^{h}_{6\Delta_1}(t_i)$, $i = m+1, m+2, ..., m+6$, where $t_i = T_1 + (i-m)\Delta_1$, $i = m+1, m+2, ..., m+6$. In the remaining intervals (i.e., $[T_1 + 6\Delta_1, T_1 + 12\Delta_1]$, $[T_1 + 12\Delta_1, T_1 + 18\Delta_1]$, $[T_1 + 18\Delta_1, T_1 + 24\Delta_1]$) we compute the Heston model forecasted log returns as expectation of the calibrated Heston model trajectories with initial condition $x_0 = x^{h}_{(k-12)\Delta_1}(t_{m+k-12})$, $v_0 = v^{h}_{(k-12)\Delta_1}(t_{m+k-12})$, $k = 12, 18, 24$. The 24 months in the future forecasted log returns after the original choice $t = T_1$ are given by $x^{h}_{24\Delta_1}(t_i) = x^{h}_{k\Delta_1}(t_i)$, $i = m+k-6, m+2, ..., m+k$, $k = 12, 18, 24$.

The results obtained in the forecasting experiment with synthetic data are shown in Figure 1. To compare the synthetic data 6 months in the future forecasts with the S&P500, 6, 12, and 24 months in the future forecasts, it is necessary to restrict the attention to a time period where all these forecasts are available. The first 24 months in the

future forecast is computed 54 months after January 2, 2009, that is, it is relative to July 5, 2013. This implies that it is chosen as the common time window of the forecasting experiments for the period July 5, 2013–January 4, 2018. In this period 55 monthly forecasts are produced. That is, despite the fact that 72 6 months in the future forecasts have been computed, the results shown in Figure 1 and in Table 1 refer to the last 55 forecasts of the 72 forecasts produced. Note that the 54 months mentioned above are obtained as 30 months of data used for the calibration of the model plus 24 months that are the projection in the future of the 24 months in the future forecast. The same choices are made when 12 months in the future forecasts are considered. That is, only the last 55 12 months in the future forecasts produced are considered in Figure 1 and Table 1. For $h = 1, 2, ..., 72$ at time $t = t^h$, the 6 months in the future Heston and oc models forecasts are obtained by calibrating the models at time $t = t^h$ (in the case of the oc model forecast choosing $T_1 = t^h$ and $T = T_1 + 6\Delta_1$). In this experiment, where the data are a numerically simulated Heston model trajectory, the Heston model forecasts are expected to be of high quality. As a consequence, when compared to the Heston model forecasts, the oc model forecasts are expected to provide a limited change in accuracy. The results shown in Figure 1 support this idea. In fact, Figure 1a shows the Heston model prices (i.e., the synthetic data), and the 6 months in the future forecasts, obtained using the calibrated Heston and oc models in the last 55 synthetic data windows considered. In Figure 1a, it is highlighted, respectively, in red and in blue the oc model forecasts that outperform or underperform the Heston model forecasts. It is shown that in approximately 49% of the cases the oc model forecasts outperform the Heston model forecasts. In the remaining cases the oc model forecasts underperform the Heston model forecasts. Figure 1b shows the frequency histogram of the relative error committed approximating the synthetic data with the corresponding 6 months in the future oc model (in the dark gray) and Heston model (in light gray) forecasts. The statistics of the relative errors is computed by dividing the interval $[0, 1]$ in 100 consecutive, nonoverlapping subintervals called "bins", of length 0.01 labeled by the index $j, j = 1, 2, ..., 100$. For $j = 1, 2, ..., 100$, to the jth bin is associated with the frequency of the event: "relative error made approximating the synthetic data in absolute value is smaller than $0.01j$, and greater or equal than $0.01(j-1)$". In the bins with label j such that $j > 47$, which are not shown in Figure 1b, the frequencies plotted in Figure 1b are zero. The histogram of Figure 1b shows that, if we look at the absolute relative error committed approximating the synthetic data with the 6 months in the future forecasts, using the oc model we obtain the relative error in absolute value smaller or equal to 3% in approximately 53% of the sample points against the 51% obtained in the same circumstances with the Heston model. Moreover, if we limit our attention to relative errors in absolute value smaller or equal to 1%, again the oc model forecast outperforms the Heston model forecasts. To evaluate more accurately the quality of the forecasts it is introduced a performance index called Conditional Mean Absolute Percentage Error (CMAPE). The CMAPE of order x, for $0 \leq x < +\infty$, is defined as the average of the absolute value of the relative errors committed approximating the prices used as data with the forecasted prices that are below the threshold x, that is,

$$\mathrm{CMAPE}(x) = \frac{\frac{1}{\mathrm{card}(\mathcal{A}_x)} \sum_{e_r \in \mathcal{A}_x} \left| e_r \right|}{\frac{\mathrm{card}(\mathcal{A}_x)}{\mathrm{card}(\mathcal{A})}}, \tag{50}$$

where e_r denotes a relative error, $\mathcal{A}$ is the set of relative errors, $\mathcal{A}_x = \{e_r \in \mathcal{A} | e_r \leq x\}$, for $0 \leq x < +\infty$. In (50) the symbols $|\cdot|$ and $\mathrm{card}(\cdot)$ denote, respectively, the absolute value of $\cdot$ and the cardinality of $\cdot$. The Mean Absolute

TABLE 1 Conditional Mean Absolute Percentage Error (CMAPE) of order x, $x = 1\%, 2\%, ..., 5\%$ and $x = +\infty$ committed approximating the simulated Heston model price with the forecasted price 6 months in the future with the oc ($\mathrm{MAPE}_{\mathrm{oc}}$) and the Heston ($\mathrm{MAPE}_{\mathrm{he}}$) models.

x(%)	$\mathrm{CMAPE}_{\mathrm{he}}(x)$(%)	$\mathrm{CMAPE}_{\mathrm{oc}}(x)$(%)	$\frac{\mathrm{CMAPE}_{\mathrm{he}}(x) - \mathrm{CMAPE}_{\mathrm{oc}}(x)}{\mathrm{CMAPE}_{\mathrm{oc}}(x)}$(%)
$+\infty$	7.80	8.49	−8.11
1	6.36	5.43	17.14
2	7.30	6.37	14.70
3	7.13	6.69	6.59
4	6.46	7.29	−11.27
5	6.44	7.38	−12.66

Abbreviations: MAPE, Mean Absolute Percentage Error; oc, optimal control; S&P500, Standard & Poor 500.

Percentage Error (MAPE) is preferred to the more usual Root Mean-Square Relative Error (RMSRE), since it is more adaptable to evaluate leptokurtic error distributions (see Karunasingha, 2022), like, the ones shown in Figures 1b, 2b, 3b, and 4b. In Tables 1–4, it is shown the CMAPE associated with the 6-month forecast for synthetic data and the 6-, 12-, and 24-month forecasts for real data. In Table 1 looking at the CMAPE($+\infty$) it is seen that the Heston model forecast slightly outperforms the oc model forecast. Needless to say CMAPE($+\infty$) is defined as $\lim_{x\to+\infty}$ CMAPE(x).

However, if the analysis is restricted to relative errors smaller or equal to x, for $x = 1\%, 2\%, ..., 5\%$, we see that the Heston model CMAPE(1%) is 17% larger than the oc model CMAPE and this difference decreases as x increases until it becomes negative when $x = 4\%, 5\%$. This shows the accuracy superiority of the oc model forecasts with respect to the Heston model forecasts when x is small. That is, the experiments suggest that, when the forecasts are close to the observations, the oc model forecasts refine the Heston model forecasts.

Moreover, the stability and sensitivity analyses of the procedures, adopted to calibrate the Heston and the oc models, are performed in the synthetic data case. The results of these analyses are shown in Tables B1–B6 of Appendix B. The variation coefficient, shown in Tables B1–B6, is defined as the standard deviation divided by the absolute value of the mean. In Table B1 the Heston model parameters used to generate the synthetic data (i.e., the "true" value row) and the summary statistics (mean, standard deviation, and variation coefficient) of the parameter estimates obtained from the calibration of the Heston model in each of the 55 data windows considered. Tables B1–B6 show the summary statistics (mean, standard deviation, and variation coefficient) of the coefficients of the quadratic polynomial that approximates, in the least-squares sense, the drift rates of the oc model obtained as solution of Problem 1 in the 55-time windows considered. For $h = 19, 20, ..., 72$, at time $t = t^h$ the coefficients of the quadratic polynomial are computed fitting, in the least-squares sense, the functions $\beta(t), \gamma(t), \delta(t), \varepsilon(t), \varphi(t)$ appearing in the optimal oc model dynamics (38) and (39) using a polynomial of degree two. Three coefficients for each approximated function and for each time $t = t^h$ considered are obtained, that is, the coefficient of the zeroth, first, and second degree terms of the approximating polynomial denoted, respectively, with a_0, a_1, a_2. Note that the variation coefficients of Heston parameters and of the coefficients of the polynomial approximation of the drift functions are small, this shows that the Heston parameters estimates and the coefficients of the polynomial approximation change slightly changing the data time window considered. These findings attest (in the numerical experiment presented) to the stability of the procedure adopted for calibrating the Heston and the oc models. Note that the means of the Heston parameter estimates reported in Table B1 are not always close to the parameter values used to generate the data. This is not unexpected, in fact the Heston calibration problem is challenging due to several reasons, including the presence of noise in the data, model assumptions, and the nonlinear nature of the model itself. As a result, discrepancies between estimated and true parameter values are not uncommon (especially, in the case of the parameters κ, θ, and v_0). Moreover, note that the

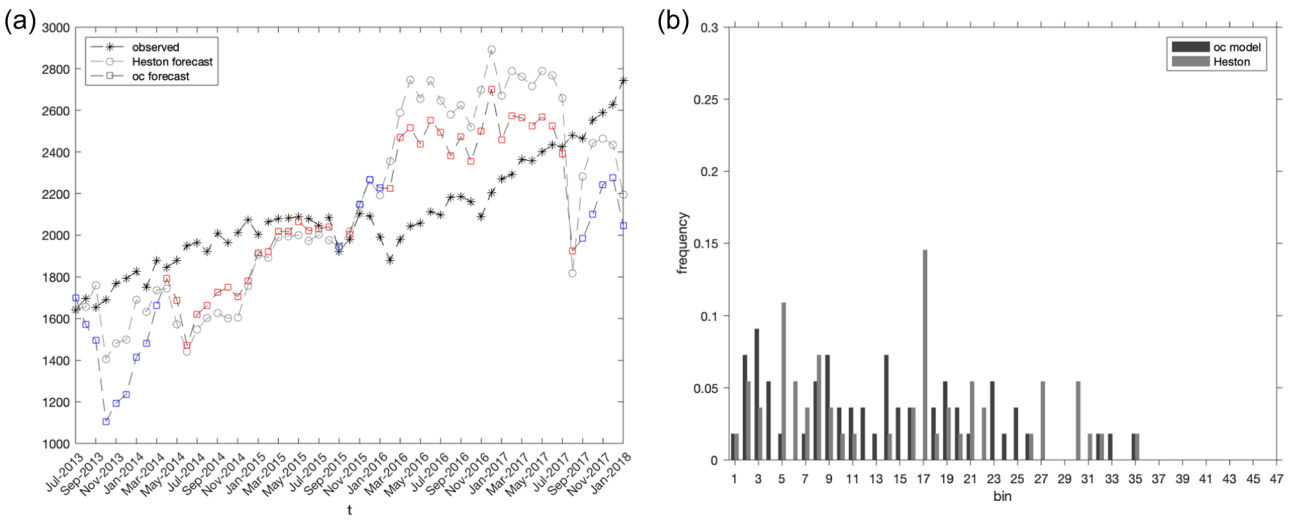

FIGURE 4 (a) Trajectory of the observed S&P500 index (-*-) and the corresponding trajectories of the forecasted S&P500 index 24 months in the future with the oc (-□-) and the Heston (-○-) models. (b) Frequency histogram of the relative errors committed approximating the observed S&P500 index with the forecasted S&P500 index 24 months in the future with the oc (in the dark gray) and the Heston (in light gray) models.

TABLE 2 Conditional Mean Absolute Percentage Error (CMAPE) of order x, $x = 1\%, 2\%, ..., 5\%$ and $x = +\infty$ committed approximating the observed S&P500 index price with the forecasted S&P500 index 6 months in the future with the oc (CMAPE_{oc}) and the Heston (CMAPE_{he}) models.

$x(\%)$	$\text{CMAPE}_{\text{he}}(x)(\%)$	$\text{CMAPE}_{\text{oc}}(x)(\%)$	$\frac{\text{CMAPE}_{\text{he}}(x) - \text{CMAPE}_{\text{oc}}(x)}{\text{CMAPE}_{\text{oc}}(x)}(\%)$
$+\infty$	4.54	3.52	28.71
1	5.41	1.83	195.0
2	4.26	2.08	104.7
3	4.01	2.24	78.76
4	3.99	2.35	69.70
5	3.94	2.58	52.78

Abbreviations: oc, optimal control; S&P500, Standard & Poor 500.

TABLE 3 Conditional Mean Absolute Percentage Error (CMAPE) of order x, $x = 1\%, 2\%, ..., 5\%$ and $x = +\infty$ committed approximating the observed S&P500 index price with the forecasted S&P500 index 12 months in the future with the oc (CMAPE_{oc}) and the Heston (CMAPE_{he}) models.

$x(\%)$	$\text{CMAPE}_{\text{he}}(x)(\%)$	$\text{CMAPE}_{\text{oc}}(x)(\%)$	$\frac{\text{CMAPE}_{\text{he}}(x) - \text{CMAPE}_{\text{oc}}(x)}{\text{CMAPE}_{\text{oc}}(x)}(\%)$
$+\infty$	9.72	7.58	28.19
1	18.34	4.21	335.7
2	22.55	4.71	378.8
3	19.19	5.00	283.7
4	17.99	6.38	181.9
5	14.92	6.43	131.9

Abbreviations: oc, optimal control; S&P500, Standard & Poor 500.

TABLE 4 Conditional Mean Absolute Percentage Error (CMAPE) of order x, $x = 2\%, 4\%, ..., 10\%$ and $x = +\infty$ committed approximating the observed S&P500 index price with the forecasted S&P500 index 24 months in the future with the oc (CMAPE_{oc}) and the Heston (CMAPE_{he}) models.

$x(\%)$	$\text{CMAPE}_{\text{he}}(x)(\%)$	$\text{CMAPE}_{\text{oc}}(x)(\%)$	$\frac{\text{CMAPE}_{\text{he}}(x) - \text{CMAPE}_{\text{oc}}(x)}{\text{CMAPE}_{\text{oc}}(x)}(\%)$
$+\infty$	2.83	2.36	10.68
2	17.87	12.69	40.75
4	14.97	4.49	57.68
6	12.74	9.43	35.10
8	11.87	10.52	12.74
10	11.58	10.98	5.51

Abbreviations: oc, optimal control; S&P500, Standard & Poor 500.

Heston parameters $k, \theta, v_0, \sigma, \rho$ shown in Table B1 as "true" values are of the same order of magnitude as those used in Duffie et al. (2000) (Table I at p. 1363) and that the correlation parameters ρ are negative, as it should be. Moreover, let us study the sensitivity of the oc model forecasts to small perturbations of the priors (i.e., to small perturbations of the values of the quantities μ, κ, θ, and x_T). That is, the values of μ, κ, θ, and x_T used in the priors are varied by a random percentage of their value. The random percentage is sampled from a uniform distribution on the interval $[-x, x]$, for $x = 5\%, 10\%, 15\%$, and we compute the resulting perturbed oc model forecasts. The corresponding functions $\beta(t), \gamma(t), \delta(t), \varepsilon(t), \varphi(t)$, appearing in the optimal oc model dynamics (38) and (39), are computed. For each sample and for each function, the MAPE of the relative difference between the perturbed and unperturbed functions is

computed. Finally, the sensitivity is measured computing, for each function, the mean MAPE of a sample made of 100 simulations. Table B7 shows the mean of MAPE of the relative difference between random perturbed and unperturbed functions $\beta(t), \gamma(t), \varepsilon(t), \varphi(t), t = t^h, h = 18, 19, ..., 72$, that is, those relative to the last 55 forecasts.

The results obtained in the forecasting experiments with real data are shown in Figures 2–4. As already mentioned, to compare the 6, 12, and 24 months forecasts it is necessary to consider a time period where the three types of forecasts are available and this time window is chosen as the period July 5, 2013–January 4, 2018. Despite the fact that we have computed 72 6-month forecasts and 66 12 months in the future forecasts, the results shown in Figures 2–4 and Tables 2–4 refer only to the last 55 forecasts computed, that is, those relative to the period July 5, 2013–January 4, 2018. Let us comment them briefly. First of all it must be said that in the interpretation of these experiments the forecasts obtained with the calibrated Heston model are used to assess the quality of the forecasts obtained with the calibrated oc model. This is due to the choice of the priors f_1^0, f_2^0 done in Section 2 and used in Problem 1. In fact, this choice implies that the calibrated oc model can be interpreted as an "enhanced" version of the Heston model. This means that, in the forecasting experiments, we expect that the performance of the calibrated oc model should "enhance" the performance of the corresponding calibrated Heston model. The results of the experiment are shown in Figures 2–4 and support this idea. For $h = 1, 2, ..., H$, in the forecasting experiments the Heston and the oc models are calibrated at time t^h and in the case of the oc model calibration we choose $T_1 = t^h$ and $T = T_1 + 6\Delta_1$ or $T = T_1 + 12\Delta_1$ or $T = T_1 + 24\Delta_1$. With these choices, we forecast at time $t = T_1 = t^h$ with the Heston and the oc model the S&P500 index log return 6, 12, and 24 months in the future, that is, 6, 12, and 24 months after time $t = T_1 = t^h, h = 1, 2, ..., H$. That is, we obtain $H = 72$ 6-months in the future forecasts, $H = 66$ 12-months in the future forecasts and $H = 55$ 24-months in the future forecasts for each one of the models (i.e., Heston and oc model) considered. In Figures 2a, 3a, and 4a the trajectory of the observed S&P500 index and the corresponding trajectories of the forecasted S&P500 index relative to the period July 5, 2013–January 4, 2018, respectively, 6, 12, and 24 months in the future obtained using the calibrated Heston and oc models are shown. In Figures 2a, 3a, and 4a, it is shown in red and in blue, respectively, the oc model forecasts that outperform and underperform the Heston forecasts. For the Heston and oc models $H = 72, 66$, and 55 calibration problems are solved corresponding to $H = 72, 66$, and 55 different data windows when $T - T_1 = 6\Delta_1$, $T - T_1 = 12\Delta_1$, $T - T_1 = 24\Delta_1$, respectively. To compare the performances of the Heston and of the oc models in the experiments the statistics (i.e., the frequency histogram) of the relative errors committed approximating the observed S&P500 index with, respectively, the 6, 12, and 24 months in the future forecasts obtained with the models considered are computed. The statistics of the relative errors of previous samples of forecasts is computed by dividing the interval $[0, 1]$ in 100 consecutive, nonoverlapping subintervals called "bins", of length 0.01 labeled by the index $j, j = 1, 2, ..., 100$. For $j = 1, 2, ..., 100$, to the jth bin is associated with the frequency of the event: "relative error made approximating the observed S&P500 index is smaller than $0.01j$, and greater or equal than $0.01(j - 1)$." In Figures 2b, 3b, and 4b, we show the frequency histograms of the relative error made approximating the observed trajectory of the S&P500 index with the S&P500 index forecasted using the Heston model (in light gray) and with the S&P500 index forecasted using the oc model (in the dark gray), respectively, 6, 12, and 24 months in the future. In the bins with label j such that $j > 47$, which are not shown in Figures 2b, 3b, and 4b, the frequencies plotted in the figures are zero. In Tables 2 and 3, it is shown the CMAPE associated, respectively, with the relative errors smaller than the threshold $x = +\infty, 1\%, 2\%, ..., 5\%$, committed approximating the observed S&P500 index, respectively, with 6 and 12 months in the future forecasts obtained with the oc and Heston models and the relative difference of the CMAPEs computed. Instead, for the 24 months in the future forecasts, Table 4 it is shown the CMAPE associated with the relative errors smaller than the threshold $x = +\infty, 2\%, 4\%, ..., 10\%$. These choices are justified by the fact that, when the forecast time horizon stretches in the future, the forecast quality decreases, and this means that, to avoid having too few relative errors smaller than the assigned threshold, it is necessary (to produce a meaningful statistics) to use bigger thresholds. First of all, let us note that the relative difference between the CMAPE$(+\infty)$ of the Heston and the oc models decreases when the forecasting horizon increases, going from 28.71% for 6 months in the future forecasts to 10.68% for 24 months in the future forecasts. Moreover, as seen for the synthetic data, the relative difference between the Heston and the oc model CMAPE(x) decreases when x increases. In particular, this difference reaches 335.7% when the relative errors of 12 months in the future forecasts smaller than 1% are considered (see Table 3). The improvement of the oc model forecasts with respect to the Heston model forecasts degrades when 24 months in the future forecasts, instead of 12 months in the future forecasts, are considered (see Table 4).

The quantitative analysis of the forecasting results presented in Tables 2–4, with the help of the CMAPE, shows that the accuracy improvement, due to the oc model, with respect to the Heston model, is greater, when $x\%$ is small, that is, when the forecasts are of high quality. Note that improving a high-quality forecast may be of great practical value, while a slightly improved low-quality forecast remains of little practical value.

Now, let us look at the forecasting results in a more qualitative way. Looking at Figures 2–4, it is easy to see that (as it should be) the quality of the forecasts of the S&P500 index degrades when we look deeper into the future. That is, the forecasted S&P500 index values 6 months in the future are of higher quality than those 12 and 24 months in the future, and the forecasted values 12 months in the future are of higher quality than those 24 months in the future. Moreover, Figures 2–4 show that the forecasted values of the S&P500 index, obtained using the oc model, are of higher quality than those obtained using the Heston model. In fact, for example, Figure 2b shows that approximately 58% of the sample points considered the relative error, committed approximating the observed S&P500 index with the forecasted S&P500 index 6 months in the future obtained with the oc model, is smaller or equal to 3%. This percentage decreases approximately to 20% and to 18% when we consider, respectively, 12 months in the future (Figure 3b) and 24 months in the future (Figure 4b) oc model forecasts.

Finally, let us present some more general comments inspired by the forecasting experiments presented in the figures. First of all, let us consider Figure 2a. In Figure 2a, we distinguish three periods corresponding to different behaviors of the observed S&P500 index, that is, the period going from June 2013 to December 2014, the period going from December 2014 to December 2015, and the period going from December 2015 to January 2018. The first and the third periods are bull markets, the second period is a kind of "correction" of the ascending trend of the S&P500 index observed in the first and third periods. In fact, in the second period the market moves laterally, in particular, this means that in the second period the market has not a definite trend. In the first period the upward trend of the S&P500 index is tracked by the two forecasted indices obtained with the calibrated Heston and oc models and the oc model does a better job than the Heston model in tracking the observed index. In the second period the observed index moves laterally and the Heston and oc model forecasts overshoot the observed index values, however, the oc model forecasts outperform the Heston model forecasts being closer to the observed index values. This behavior is more evident when we look at deeper in the future forecasts (i.e., 12 and 24 months in the future forecasts shown, respectively, in Figures 3a and 4a). In the second period the forecasts, obtained with the oc model, are less accurate than those obtained in the first period. This is due to the fact that the calibrated Heston and oc models, that are used to produce the forecasts of the second period, use as calibration data the data (at least in part) relative to the bull market of the first period. That is, in some sense, in the second period and, in particular, at the beginning of the second period the calibrated oc models used to produce the forecasts are "bullish" while the market is moving laterally. A similar behavior is observed for the Heston model forecasts in the second period. Finally, in the third period the S&P500 index starts to rise again. Figure 2a shows that, at the beginning of the third period, the oc model underperforms the Heston model and underestimates the observed index. However, during the third period after a while the oc model comes back and becomes more accurate than the Heston model in forecasting the S&P500 index. The unsatisfactory behavior of the oc model at the beginning of the third period is due to the fact that the oc model, that in the second period has tracked the lateral trend of the index more closely than the Heston model, needs more time than the Heston model to adjust its forecasts when, in the third period, a new bull market starts. Similarly, it is understandable that the Heston model, which in the second period, has underperformed the oc model in the overshooting of the observed S&P500 index, is quicker than the oc model in adapting its forecasts to the observed index when in the third period a new bull market starts. It is easy to see that the previous analysis based on Figure 2a is confirmed by Figures 3a and 4a.

The results shown in Figures 2–4 support the idea that the oc model resulting from the calibration problem discussed in Section 2 can be seen as an enhanced version of the Heston model.

4 | CONCLUSIONS

In this paper, it is considered a "real world" calibration problem of a partially specified stochastic volatility model called the oc model. In this model the asset price drift rate and the stochastic variance drift are unknown functions. These functions are determined solving the oc model calibration problem. This is done using as data a set of observed asset log returns, their observation times and solving a preliminary calibration problem for the Heston model. The oc model calibration problem is formulated as a stochastic optimal control problem that is solved using the dynamic programming principle. Two priors suggested by the Heston model are used in the oc model

calibration procedure. The oc model and the Heston model are calibrated with synthetic and real data, that is, S&P500 data, and the calibrated models are used to produce 6 months in the future forecasts and S&P500 6, 12, and 24 months in the future forecasts. The robustness, stability and sensitivity analyses of the oc model calibration procedures are also performed using synthetic data. The oc model presented in this paper can be seen as an enhanced version of the Heston model. The study of the oc model, when compared to the study of the Heston model, requires more advanced analytical techniques (i.e., stochastic optimal control and dynamic programming) along with an increased computational effort. However, the results of the numerical experiments shown in Section 3 confirm the improved accuracy of the oc model forecasts with respect to the Heston model forecasts both from the qualitative and quantitative standpoints. The quantitative assessment of the forecasting results presented in Tables 2–4 shows that the accuracy improvement due to the use of the oc model, rather than the Heston model, is greatest when the forecasts are of high quality (i.e., when $x\%$ is small). That is, the most significant accuracy enhancements due to the use of the oc model occur when the Heston forecasts are close to the observations, that is, when the Heston forecasts are successful. This is a very valuable feature in practical circumstances. Moreover, Figures 2a 3a, and 4a show that, in simple market situations, that is, for example, when the market has a definite trend (i.e., it is a bull market in the experiments presented), high-quality S&P500 index forecasts can be obtained from the calibrated Heston and oc models in the case of 6 and 12 months in the future forecasts (Figures 3a and 4a). The 24 months in the future forecasts shown in Figure 4a are of low quality. Figures 2a, 3a, and 4a (in particular the 24 months in the future forecasts shown in Figure 4a) show that the asset price dynamics forecasted by the oc and Heston models commits a kind of "nonconstant systematic error". That is, the error committed is not always the same but depends (in a simple manner) on the circumstances (i.e., in the experiment presented depends on the circumstance that a lateral market follows a bull market). This kind of error can be successfully handled complementing the results shown here, obtained with stochastic volatility models, with those obtained with the techniques coming from data science and machine learning. This last idea together with some hints coming from the emerging field of generative Artificial Intelligence (AI) is susceptible of interesting developments. Indeed, the integration of generative AI techniques with stochastic volatility models presents an exciting subject for further research. Generative AI models, such as Generative Adversarial Networks or Variational Autoencoders, have shown promise in capturing complex data distributions and generating realistic synthetic data. In the context of forecasting, generative AI techniques could be employed to simulate alternative scenarios and to capture the inherent uncertainty in financial markets. Furthermore, combining generative AI with stochastic volatility models may be the right combination of tools to address the "nonconstant systematic error" mentioned above. The generative models can potentially capture the variability in the error term and generate forecasts that account for changing market conditions or circumstances. However, it is important to note that integrating stochastic volatility models and generative AI with financial forecasting is still an unexplored field, and there are challenges to be addressed. These include data quality and availability, model interpretability, and ensuring the generated scenarios align with economic and financial principles. Overall, the investigation of the potential of stochastic volatility models and of the generative AI techniques in producing more precise forecasts is a valid and possibly fruitful research field.

DATA AVAILABILITY STATEMENT

Research data are not shared. The data that support the findings of this study are available from the Refinitiv Eikon database. Restrictions apply to the availability of these data, which were used under license for this study.

ORCID

Francesca Mariani http://orcid.org/0000-0002-4068-3411

REFERENCES

Aït-Sahalia, Y., Fan, J., & Li, Y. (2013). The leverage effect puzzle: Disentangling sources of bias at high frequency. *Journal of Financial Economics*, *109*, 224–249.

Amengual, D., & Xiu, D. (2018). Resolution of policy uncertainty and sudden declines in volatility. *Journal of Econometrics*, *203*(2), 297–315.

Andersen, L. B. G. (2008). Simple and efficient simulation of the Heston stochastic volatility model. *Journal of Computational Finance*, *11*, 1–42.

Andersen, L. B. G., & Piterbarg, V. V. (2007). Moment explosions in stochastic volatility models. *Finance and Stochastic*, *11*, 29–50.

Avellaneda, M., Friedman, C., Holmes, R., & Samperi, D. (1997). Calibrating volatility surfaces via relative-entropy minimization. *Applied Mathematical Finance*, *4*(1), 37–64.
Baillie, R. T., & De Gennaro, R. (1990). Stock returns and volatility. *Journal of Financial and Quantitative Analysis*, *25*(2), 203–214.
Bibby, B. M., & Sørensen, M. (1995). Martingale estimation functions for discretely observed diffusion processes. *Bernoulli*, *1*(1/2), 17–39.
Black, F. (1976). Studies of stock price volatility changes. In *Proceedings of the 1976 Meeting of the Business and Economics Statistics Section, American Statistical Association*, 177–181.
Broadie, M., Chernov, M., & Johannes, M. (2007). Model specification and risk premiums: The evidence from the futures options. *Journal of Finance*, *62*(3), 1453–1490.
Campbell, J. Y., & Hentschel, L. (1991). No news is good news: An asymmetric model of changing volatility in stock returns. *Journal of Financial Economics*, *31*(3), 281–318.
Carmona, R., & Xu, L. (1997). *Calibrating arbitrage-free stochastic volatility models by relative entropy method* (Civil Engineering and Operations Research (CEOR) Technical Report). Princeton University.
Christie, A. (1982). The stochastic behavior of common stock variances: Value, leverage, and interest rate effects. *Journal of Financial Economics*, *10*, 407–432.
Duffie, D., Pan, J., & Singleton, K. (2000). Transform analysis and asset pricing for affine jump-diffusions. *Econometrica*, *68*, 1343–1376.
Fatone, L., Mariani, F., Recchioni, M. C., & Zirilli, F. (2008). The calibration of the Heston stochastic volatility model using filtering and maximum likelihood methods. In G. S. Ladde, N. G. Medhin, C. Peng, & M. Sambandham (Eds.), *Proceedings of the Dynamic Systems and Applications* (Vol. 5, pp. 170–181). Dynamic Publishers.
Fatone, L., Mariani, F., Recchioni, M. C., & Zirilli, F. (2014). The calibration of some stochastic volatility models used in mathematical finance. *Open Journal of Applied Sciences*, *4*, 23–33.
Feller, W. (1951). Two singular diffusion problems. *Annals of Mathematics*, *54*, 173–182.
French, K. R., Schwert, G., & Stambaugh, R. F. (1987). Expected stock returns and volatility. *Journal of Financial Economics*, *19*(1), 3–29.
Gatheral, J. (2006). *The volatility surface: A practitioner's guide*. Wiley Finance, John Wiley & Sons.
Heston, S. (1993). A closed form solution for options with stochastic volatility with applications to bond and currency options. *Review of Financial Studies*, *6*(2), 327–344.
Karunasingha, D. S. K. (2022). Root mean square error or mean absolute error? Use their ratio as well. *Information Sciences*, *585*, 609–629.
Kolosov, G. E. (1999). *Optimal design of control systems: Stochastic and deterministic problems*. CRC Press.
Kloeden, P. E., & Platen, E. (1992). *Numerical solution of stochastic differential equations*. Springer-Verlag.
Ladd, A. J. C., & Szymczak, P. (2003). Boundary conditions for stochastic solutions of the convection-diffusion equation. *Physical Review E*, *68*, 036704.
Mariani, F., Pacelli, G., & Zirilli, F. (2008). Maximum likelihood estimation of the Heston stochastic volatility model using asset and option prices: An application of nonlinear filtering theory. *Optimization Letters*, *2*(2), 177–222.
Nayak, S., & Papanicolaou, G. (2007). *Stochastic volatility surface estimation*. Preprint available on http://math.stanford.edu/papanico/pubftp/svcalp3.pdf
Pacati, C., Pompa, G., & Renò, R. (2018). Smiling twice: The Heston++ model. *Journal of Banking and Finance*, *96*, 185–206.
Song, Z., & Xiu, D. (2016). A tale of two option markets: State-price densities and volatility risk. *Journal of Econometrics*, *190*, 176–196.
Wilmott, P. (1998). *Derivatives. The theory and practice of financial engineering*. John Wiley & Sons.

How to cite this article: Fatone, L., Mariani, F., & Zirilli, F. (2024). Calibration in the "real world" of a partially specified stochastic volatility model. *The Journal of Futures Markets*, *44*, 75–102. https://doi.org/10.1002/fut.22461

APPENDIX A

Let us list some useful formulae. Let $\underline{e}_i$, $i = 1, 2, ..., n$, be the canonical basis vectors of $\mathbb{R}^6$. The matrices $D, E(\underline{k})$, $\underline{k} = [k_1, k_2, ..., k_6]^\top \in \mathbb{R}^6$, and the vector $\underline{b} \in \mathbb{R}^6$, that appear in (22) are given by

$$D = \begin{bmatrix} 0 & -k\theta & 0 & 0 & -\mu & 0 \\ 0 & k & -(\sigma^2 + 2k\theta) & -(\mu + \sigma\rho) & \frac{1}{2} & -1 \\ 0 & 0 & 2k & \frac{1}{2} & 0 & 0 \\ 0 & 0 & 0 & k & 0 & 1 \\ 0 & 0 & 0 & -k\theta & 0 & -2\mu \\ 0 & 0 & 0 & 0 & 0 & 0 \end{bmatrix}, \tag{A1}$$

$$E(\underline{k}) = \begin{bmatrix} -\frac{1}{2w_3}\underline{k}^\top \underline{e}_2 \underline{e}_2^\top - \frac{1}{2w_2}\underline{k}^\top \underline{e}_5 \underline{e}_5^\top \\ -\frac{2}{w_3}\underline{k}^\top \underline{e}_2 \underline{e}_3^\top - \frac{1}{w_2}\underline{k}^\top \underline{e}_2 \underline{e}_4^\top \\ -\frac{2}{w_3}\underline{k}^\top \underline{e}_3 \underline{e}_3^\top - \frac{1}{2w_2}\underline{k}^\top \underline{e}_4 \underline{e}_4^\top \\ -\frac{2}{w_3}\underline{k}^\top \underline{e}_3 \underline{e}_4^\top - \frac{2}{w_2}\underline{k}^\top \underline{e}_4 \underline{e}_6^\top \\ -\frac{1}{w_3}\underline{k}^\top \underline{e}_2 \underline{e}_4^\top - \frac{2}{w_2}\underline{k}^\top \underline{e}_5 \underline{e}_6^\top \\ -\frac{1}{2w_3}\underline{k}^\top \underline{e}_4 \underline{e}_4^\top - \frac{2}{w_2}\underline{k}^\top \underline{e}_6 \underline{e}_6^\top \end{bmatrix}, \quad \underline{k} \in \mathbb{R}^6, \tag{A2}$$

$$\underline{b}(t) = \left[\frac{w_1}{2}\tilde{x}^2(t), 0, 0, 0, -w_1\tilde{x}(t), \frac{w_1}{2}\right]^\top, \quad t \in [0, T]. \tag{A3}$$

The matrices D_p and $E_p(\underline{k})$, $\underline{k} \in \mathbb{R}^6$, $0 \le p \le 1$, of (30) are given, respectively, by

$$D_p = \begin{bmatrix} 0 & -k\theta & 0 & 0 & -\mu & 0 \\ 0 & k & -(\sigma^2 + 2k\theta) & -(\mu + \sigma\rho) & \frac{p}{2} & -p \\ 0 & 0 & 2k & \frac{p}{2} & 0 & 0 \\ 0 & 0 & 0 & k & 0 & p \\ 0 & 0 & 0 & -k\theta p & 0 & -2\mu \\ 0 & 0 & 0 & 0 & 0 & 0 \end{bmatrix}, \quad 0 \le p \le 1, \tag{A4}$$

$$E_p(\underline{k}) = \begin{bmatrix} -\frac{1}{2w_3}\underline{k}^\top \underline{e}_2 \underline{e}_2^\top - \frac{1}{2w_2}\underline{k}^\top \underline{e}_5 \underline{e}_5^\top \\ -\frac{2}{w_3}\underline{k}^\top \underline{e}_2 \underline{e}_3^\top - \frac{p}{w_2}\underline{k}^\top \underline{e}_2 \underline{e}_4^\top \\ -\frac{2}{w_3}\underline{k}^\top \underline{e}_3 \underline{e}_3^\top - \frac{p}{2w_2}\underline{k}^\top \underline{e}_4 \underline{e}_4^\top \\ -\frac{2}{w_3}\underline{k}^\top \underline{e}_3 \underline{e}_4^\top - \frac{2}{w_2}\underline{k}^\top \underline{e}_4 \underline{e}_6^\top \\ -\frac{p}{w_3}\underline{k}^\top \underline{e}_2 \underline{e}_4^\top - \frac{2}{w_2}\underline{k}^\top \underline{e}_5 \underline{e}_6^\top \\ -\frac{p}{2w_3}\underline{k}^\top \underline{e}_4 \underline{e}_4^\top - \frac{2}{w_2}\underline{k}^\top \underline{e}_6 \underline{e}_6^\top \end{bmatrix}, \quad \underline{k} \in \mathbb{R}^6, \quad 0 \le p \le 1. \tag{A5}$$

In particular when $p = 0$ the matrices D_0 and $E_0(\underline{k})$, $\underline{k} \in \mathbb{R}^6$, of (33) are given by

$$D_0 = \begin{bmatrix} 0 & -k\theta & 0 & 0 & -\mu & 0 \\ 0 & k & -(\sigma^2 + 2k\theta) & -(\mu + \sigma\rho) & 0 & 0 \\ 0 & 0 & 2k & 0 & 0 & 0 \\ 0 & 0 & 0 & k & 0 & 0 \\ 0 & 0 & 0 & 0 & 0 & -2\mu \\ 0 & 0 & 0 & 0 & 0 & 0 \end{bmatrix}, \tag{A6}$$

$$E_0(\underline{k}) = \begin{bmatrix} -\frac{1}{2w_3}\underline{k}^\top \underline{e}_2 \underline{e}_2^\top - \frac{1}{2w_2}\underline{k}^\top \underline{e}_5 \underline{e}_5^\top \\ -\frac{2}{w_3}\underline{k}^\top \underline{e}_2 \underline{e}_3^\top \\ -\frac{2}{w_3}\underline{k}^\top \underline{e}_3 \underline{e}_3^\top \\ -\frac{2}{w_3}\underline{k}^\top \underline{e}_3 \underline{e}_4^\top - \frac{2}{w_2}\underline{k}^\top \underline{e}_4 \underline{e}_6^\top \\ -\frac{2}{w_2}\underline{k}^\top \underline{e}_5 \underline{e}_6^\top \\ -\frac{2}{w_2}\underline{k}^\top \underline{e}_6 \underline{e}_6^\top \end{bmatrix}, \quad \underline{k} \in \mathbb{R}^6. \tag{A7}$$

The matrix $F_1(\underline{k})$, $\underline{k} = [k_1, k_2, ..., k_6]^\top \in \mathbb{R}^6$, and the vector $\underline{b}_1(\underline{k})$, $\underline{k} \in \mathbb{R}^6$, of (35) are given by

$$F_1(\underline{k}) = \begin{bmatrix} 0 & -\frac{k_2}{w_3} - k\theta & 0 & 0 & -\mu - \frac{k_5}{w_2} & 0 \\ 0 & k - \frac{2k_3}{w_3} & -(\sigma^2 + 2k\theta) - \frac{2k_2}{w_3} & 0 & 0 & 0 \\ 0 & 0 & 2k - \frac{4k_3}{w_3} & 0 & 0 & 0 \\ 0 & 0 & 0 & k - \frac{2k_6}{w_2} & 0 & -\frac{2k_4}{w_2} \\ 0 & 0 & 0 & -k\theta & -\frac{2k_6}{w_2} & -2\mu - \frac{2k_5}{w_2} \\ 0 & 0 & 0 & 0 & 0 & -\frac{4k_6}{w_2} \end{bmatrix}, \quad \underline{k} \in \mathbb{R}^6, \tag{A8}$$

$$b_1(\underline{k}) = \left[0, -(\mu + \sigma\rho)k_4 + \frac{1}{2}k_5 - k_6 - \frac{1}{w_2}k_2k_4, \frac{1}{2}k_4 - \frac{1}{2w_2}k_4^2, k_6, -\frac{1}{w_3}k_2k_4, -\frac{1}{2w_3}k_4^2\right]^\top, \tag{A9}$$

where $\underline{k} = [k_1, k_2, k_3, k_4, k_5, k_6]^\top \in \mathbb{R}^6$.

APPENDIX B

Let us show below some tables and figures useful to evaluate the results obtained in the numerical experiments about the stability and sensitivity analyses of the calibration procedures of the Heston and oc models (Tables B1–B7).

TABLE B1 Summary statistics ("true" value, i.e., the value used to generate the data, mean, standard deviation, and variation coefficient of the quantities estimated in the numerical experiments) for the Heston parameters obtained from the calibration of the synthetic data.

	μ	κ	θ	v_0	σ	ρ
"True" value	**0.1306**	**2.5617**	**0.0581**	**0.4403**	**0.3831**	**−0.3743**
Mean	0.1281	1.6136	0.0802	0.0856	0.2078	−0.2190
SD	0.0264	1.1356	0.0269	0.2710	0.1305	0.1506
Variation coefficient	0.2168	0.5865	1.1772	2.7712	0.6199	−0.5898

Note: The first row of the table contains the Heston parameters used to generate the synthetic data.

TABLE B2 Summary statistics (mean, standard deviation, and variation coefficient of the quantities estimated in the numerical experiments) for the coefficients of the quadratic polynomial approximating the functions $\beta(t)$, $t = t^h$, $h = 18, 19, ..., 72$.

	a_0	a_1	a_2
Mean	−6.139e − 03	3.541e − 06	−7.856e − 04
SD	4.936e − 03	1.465e − 05	3.361e − 08
Variation coefficient	0.8041	4.1401	0.6844

TABLE B3 Summary statistics (mean, standard deviation, and variation coefficient of the quantities estimated in the numerical experiments) for the coefficients of the quadratic polynomial approximating the functions $\gamma(t)$, $t = t^h$, $h = 18, 19, ..., 72$.

	a_0	a_1	a_2
Mean	1.534e − 06	1.534e − 06	3.431e − 08
SD	8.939e − 04	3.919e − 06	5.260e − 09
Variation coefficient	1.1379	2.5554	1.5334

TABLE B4 Summary statistics (mean, standard deviation, and variation coefficient of the quantities estimated in the numerical experiments) for the coefficients of the quadratic polynomial approximating the functions $\delta(t)$, $t = t^h$, $h = 18, 19, ..., 72$.

	a_0	a_1	a_2
Mean	3.265e − 03	3.313e − 06	−4.151e − 08
SD	2.269e − 03	2.883e − 06	2.594e − 08
Variation coefficient	0.6949	0.8700	0.6250

TABLE B5 Summary statistics (mean, standard deviation, and variation coefficient of the quantities estimated in the numerical experiments) for the coefficients of the quadratic polynomial approximating the functions $\varepsilon(t)$, $t = t^h$, $h = 18, 19, ..., 72$.

	a_0	a_1	a_2
Mean	−2.632e − 04	2.366e − 05	5.493e − 08
SD	0.8453e − 03	0.0176e − 03	4.39e − 08
Variation coefficient	3.2113	0.7431	0.7992

TABLE B6 Summary statistics (mean, standard deviation, and variation coefficient of the quantities estimated in the numerical experiments) for the coefficients of the quadratic polynomial approximating the functions $\varphi(t)$, $t = t^h$, $h = 18, 19, ..., 72$.

	a_0	a_1	a_1
Mean	−6.128e − 03	−1.073e − 05	6.927e − 08
SD	3.53e − 03	6.182e − 06	3.990e − 08
Variation coefficient	0.576	0.576	0.576

TABLE B7 Mean of MAPE of the relative difference between random perturbed and unperturbed functions: $\beta(t)$, $\gamma(t)$, $\delta(t)$, $\varepsilon(t)$, $\varphi(t)$, for $t = t^h$, $h = 18, 19, ..., 72$, when the percentage of perturbation $x = 5\%, 10\%, 15\%$.

x (%)	β(%)	γ(%)	δ(%)	ε(%)	φ(%)
5	0.53 (10.6)	1.71 (34.2)	0.74 (14.8)	16.4 (3.28)	4.5e − 04 (8.9e − 3)
10	1.05 (10.5)	3.34 (33.4)	1.47 (14.7)	32.8 (3.28)	8.8e − 04 (8.9e − 3)
15	1.57 (10.4)	4.93 (32.87)	2.18 (14.5)	49.3 (3.29)	1.3e − 03 (8.7e − 3)

Note: In the brackets the mean as percentage of x.

Abbreviation: MAPE, Mean Absolute Percentage Error.